Engineering E. coli for the biosynthesis of 3-hydroxy-#-butyrolactone (3HBL) and 3,4-dihydroxybutyric acid (3,4-DHBA) as value-added chemicals from glucose as a sole carbon source

Citation: Dhamankar, Himanshu, Yekaterina Tarasova, Collin H. Martin, and Kristala L.J. Prather. "Engineering E. Coli for the Biosynthesis of 3-Hydroxy-γ-Butyrolactone (3HBL) and 3,4-Dihydroxybutyric Acid (3,4-DHBA) as Value-Added Chemicals from Glucose as a Sole Carbon Source." Metabolic Engineering 25 (September 2014): 72–81.

As Published: http://dx.doi.org/10.1016/j.ymben.2014.06.004

Publisher: Elsevier

Persistent URL: http://hdl.handle.net/1721.1/101387

Version: Author's final manuscript: final author's manuscript post peer review, without publisher's formatting or copy editing

Engineering *E. coli* for the biosynthesis of 3-hydroxy-γ-butyrolactone (3HBL) and 3,4-dihydroxybutyric acid (3,4-DHBA) as value-added chemicals from glucose as a sole carbon source

Himanshu Dhamankar[a,b], Yekaterina Tarasova[b,c], Collin H. Martin[a,b,1], Kristala L. Jones Prather[a,b,*]

[a] *Department of Chemical Engineering, Massachusetts Institute of Technology, Cambridge, MA 02139*

[b] *Synthetic Biology Engineering Research Center (SynBERC), Massachusetts Institute of Technology, Cambridge, MA 02139*

[c] *Microbiology Graduate Program, Massachusetts Institute of Technology, Cambridge, MA 02139*

Submitted for publication in: ***Metabolic Engineering***

[1]Current address:

The Dow Chemical Company, Spring House, PA 19477, USA

* Corresponding author:

Department of Chemical Engineering

77 Massachusetts Avenue, Room E17-504

Cambridge, MA 02139

Phone: 617.253.1950

Fax: 617.258.5042

Email: kljp@mit.edu

Keywords: 3-hydroxy-γ-buytrolactone, hydroxyacids, glycolate, glyoxylate shunt, T7 RNAP based expression, orthogonal expression systems, metabolic burden

Abstract

3-hydroxy-γ-butyrolactone (3HBL) is a versatile chiral synthon, deemed a top value-added chemical from biomass by the DOE. We recently reported the first biosynthetic pathway towards 3HBL and its hydrolyzed form, 3,4-dihydroxybutyric acid (3,4-DHBA) in recombinant *Escherichia coli* using glucose and glycolic acid as feedstocks and briefly described their synthesis solely from glucose. Synthesis from glucose requires integration of the endogenous glyoxylate shunt with the 3,4-DHBA/3HBL pathway and co-overexpression of seven genes, posing challenges with respect to expression, repression of the glyoxylate shunt and optimal carbon distribution between the two pathways. Here we discuss engineering this integration. While appropriate media and over-expression of glyoxylate shunt enzymes helped overcome repression, two orthogonal expression systems were employed to address the expression and carbon distribution challenge. Synthesis of up to 0.3 g/L of 3HBL and 0.7 g/L of 3,4-DHBA solely from glucose was demonstrated, amounting to 24% of the theoretical maximum.

1. Introduction

3-Hydroxy-γ-butyrolactone (3HBL) is a versatile chiral C4 building block with applications in the synthesis of a variety of pharmaceuticals, polymers and solvents (Werpy and Peterson, 2004). In particular, *(S)*-3-hydroxy-γ-butyrolactone can serve as a precursor to various enantiopure intermediates for chiral drugs such as the cholesterol-reducing statins like Lipitor® (Pfizer) and Crestor® (AstraZeneca), antibiotics such as carbapenems and linezolid (Zyvox®), and the anti-hyperlipidemic medication Zetia® (Lee and Park, 2009). Artovastatin (the active ingredient in Lipitor®) is synthesized via hydroxynitrile, an intermediate which may be readily synthesized from *(S)*-3HBL. Both *(R)*-3HBL and *(S)*-3HBL may be used in the synthesis of the nutritional supplement L-carnitine (Byun et al., 2002; Hwang et al., 2009). Further, the alcohol and acid functional groups in *(S)*-3HBL can be derivatized to yield various substituted tetrahydrofurans, amides, lactones, nitriles and epoxides that may in turn serve as chiral building blocks (Furrow et al., 1998; Wang and Hollingsworth, 1999; Yang et al., 2012) and solvents (Werpy and Peterson, 2004).

Owing to these numerous applications, 3HBL has been identified as one of the top value-added chemicals from biomass in a report by the U.S. Department of Energy (Werpy and Peterson, 2004). While numerous chemical and chemo-enzymatic routes have been reported towards 3HBL (Lee and Park, 2009), these suffer from various disadvantages including expensive or hazardous starting materials and reagents, harsh processing conditions and poor yields and selectivity resulting in cost prohibitive separation processes (Kumar et al., 2005; Nakagawa et al., 2006; Park et al., 2004; Shin et al., 2005; Suzuki et al., 1999). In contrast, biological processes employ mild conditions and safer raw materials, afford high selectivity, and may hence offer an economically viable route for the synthesis of this valuable chemical.

We recently reported the biosynthesis of 3HBL and its free acid form, 3,4-dihydroxybutyric acid (3,4-DHBA) using glycolic acid and glucose as starting materials via our *de novo* constructed 3-hydroxyacid (3HA) platform pathway (Martin et al., 2013; **Figure 1**). The 3HA platform allows synthesis of various 3-hydroxyacids of desired carbon chain lengths and substituents, using different small acid molecules as starting substrates. In the synthesis of 3,4-DHBA and 3HBL, glycolic acid fed to the cells is activated intracellularly to glycolyl-CoA by the enzyme propionyl coenzyme A transferase (Pct, coded by the *pct* gene from *Megasphaera elsdenii*) that transfers coenzyme A (CoA) from a molecule of acetyl-CoA to glycolate. Glycolyl-CoA further undergoes a Claisen condensation reaction (Masamune et al., 1989) with acetyl-CoA, catalyzed by the biosynthetic thiolase BktB (from *Cupriavidus necator*) to form 3-keto-4-hydroxybutyryl-CoA, followed by stereospecific reduction by the PhaB reductase (from *C. necator*) to *(S)*-3,4-dihydroxybutyryl-CoA. TesB, the endogenous thioesterase II enzyme from *E. coli* can then be used for CoA removal by cleavage of the thioester bond in *(S)*-3,4-dihydroxybutyryl-CoA to obtain *(S)*-3,4-dihydroxybutyric acid (3,4-DHBA). 3,4-DHBA, thus synthesized by the recombinant *E. coli* cells is secreted into the culture medium and can be readily lactonized to 3HBL via a simple acid treatment. The pathway also directly yields 3HBL formed due to spontaneous and/or host enzyme-catalyzed lactonization of the 3,4-dihydroxybutyryl-CoA intermediate (Martin et al., 2013). Using this pathway, we have now synthesized up to 918 ± 21 mg/L of *(S)-3,4*-DHBA and 271 ± 15 mg/L of *(S)*-3HBL (10.3 mM total titers) using a recombinant *E. coli* K-12 strain (MG1655 (DE3)) expressing the various pathway enzymes in cultures supplemented with 1% glucose and 40 mM glycolate (**Supplementary Figure S1**). Depending on the sequential order of reaction of the two thioesters in the active site of BktB, the condensation reaction between glycolyl-CoA and acetyl-CoA takes place in two ways (Martin et al., 2013), resulting in the synthesis of up to 1357 ± 28 mg/L of the 2,3-dihydroxybutyric acid (2,3-DHBA) isomer in addition to 3,4-DHBA. Similarly, up to 678 ± 33 mg/L of 3-hydroxybutyric acid (3HB) and 1802 ± 84 mg/L of acetate are produced as inevitable pathway side products (**Figure 1**).

Glycolate itself may be synthesized in *E. coli* from glyoxylate by the enzyme glyoxylate reductase, encoded by the endogenous *ycdW* gene. Endogenous synthesis of glycolate from glucose in cells expressing the 3,4-DHBA/3HBL pathway enzymes can allow direct synthesis of these molecules from glucose as a single carbon source, eliminating the need to supply glycolic acid as a separate feedstock. In addition to mitigating cost, such intracellular glycolate synthesis is also expected to overcome any limitations in pathway yield and productivity associated with the transport of exogenously supplied glycolate across the cell membrane and boost intracellular glycolate and glycolyl-CoA levels, improving selectivity and productivity. Further, direct synthesis of 3,4-DHBA and 3HBL from substrates such as glucose opens avenues towards the synthesis of these valuable chemicals from other simple sugars derived from biomass.

In wild type *E. coli,* the glyoxylate shunt (**Supplementary Figure S2a**) is heavily regulated and is only active during growth on acetate or fatty acids where it is required for carbon assimilation for synthesis of cell building blocks (Cozzone, 1998). It is repressed during growth on glucose or in rich medium (such as LB). Such a binary response to changes in available fermentable sugars and metabolites is achieved by controlling the expression of the enzymes of the glyoxylate shunt (AceA, AceB and AceK) and by re-directing part of the flux of isocitrate from the TCA cycle to the glyoxylate shunt by reducing the activity of isocitrate dehydrogenase (Idh, coded by the gene *icd*) through reversible phosphorylation by Idh kinase/phosphatase (AceK) (Laporte and Koshland, 1982). Expression of the *aceBAK* operon is regulated at the transcriptional level by the repressor protein IclR. During growth on acetate or fatty acids, this repression by IclR is relieved, and phosphorylation of Idh by AceK results in a drastic drop in its activity. Simultaneously, expression of isocitrate lyase (AceA) which catalyzes the cleavage of isocitrate into glyoxylate and succinate, results in re-directing the isocitrate flux towards the glyoxylate shunt. On the other hand, changes in the levels of metabolites in the presence of glucose or other readily fermentable sugars result in dephosphorylation of Idh by AceK

(Nimmo and Nimmo, 1984), thereby activating Idh and diverting the isocitrate flux back through the TCA cycle.

To achieve glycolate synthesis from glucose via the glyoxylate shunt, we investigated different approaches to overcome this endogenous repression, such as the use of two different culture media (LB vs M9), varying the glucose supplementation, over-expression of the enzymes of the glyoxylate shunt and enhancing endogenous expression of the *aceBAK* operon by knocking out the transcriptional regulator *iclR*. Further, glyoxylate and glycolate synthesized endogenously can be readily metabolized into a number of cell building blocks such as malate, 3-phosphoglycerate and 2-keto-4-hydroxyglutarate via a number of competing pathways (**Supplementary Figure S2b**). As part of this study, we also investigated the effect of knocking out some of these competing pathways on glycolate and DHBA/3HBL synthesis.

Integration of the glycolate and 3,4-DHBA/3HBL pathways requires the simultaneous over-expression of seven different pathway enzymes, imposing considerable metabolic stress. In addition to overcoming the endogenous repression of the glyoxylate shunt, achieving expression of all pathway enzymes and controlling the distribution of carbon between the two pathways is critical for effective product synthesis and improving pathway yield. In Martin *et al.* (2013), we presented some preliminary data for such direct synthesis of 3HBL from glucose. It is our objective in this manuscript to discuss the different challenges encountered and strategies employed to engineer the integration of these pathways for the construction of an *E. coli* strain capable of endogenous glycolate, 3,4-DHBA and 3HBL synthesis from glucose as a sole carbon source. Finally, one mole of acetate is produced per mole of 3,4-DHBA synthesized as a by-product of the activation reaction of glycolate to glycolyl-CoA by Pct. Recycling this acetate back to acetyl-CoA using acetyl-CoA synthetase is expected to increase the acetyl-CoA availability for product synthesis and improve the overall pathway yield. The effect of over-expression of acetyl-CoA synthetase on the product titers and overall pathway yield was also assessed.

2. Materials and Methods

2.1. *Microbial strains and plasmids* (Table 1)

Table 1 lists the various strains and plasmids used in this study. The *E. coli* MG1655 (DE3) strain (Tseng et al., 2009), allows expression of various pathway genes cloned into Duet vectors (Novagen, Darmstadt, Germany) upon induction with isopropyl β-D-1-thiogalactopyranoside (IPTG). This strain served as the host strain for subsequent chromosomal modifications for construction of various glycolate producing strains. *E.coli* DH10B (Invitrogen, Carlsbad, CA) and ElectroTen-Blue (Stratagene, La Jolla, CA) electrocompetent cells were used for transformation with ligation reactions and propagation of all plasmids.

The two co-replicable plasmids, pDHP-1 (pETDuet/bktB/phaB) and pDHP-2 (pCDFDuet/pct/tesB) were previously constructed for expression of *bktB*, *phaB*, *pct* and *tesB* for the 3,4-DHBA and 3HBL synthesis pathway (Martin et al., 2013). Both of these plasmids contain the respective pathway genes cloned downstream of T7*lac* promoters and ribosome binding sites in the respective Duet vectors. The *ycdW* gene was cloned between the NdeI and XhoI sites in MCSII of pCOLADuet-1 to first construct pCOLADuet-*ycdW*. The *aceA-aceK* genes from the *aceBAK* operon were amplified with flanking NcoI and EcoRI restriction sites via polymerase chain reaction (PCR) using MG1655 (DE3) genomic DNA (gDNA) as template and cloned into MCSI between the NcoI and EcoRI sites of pCOLADuet-*ycdW* to construct pGLY-1. The primers used to amplify different fragments for cloning reactions are listed in **Supplementary Table S1.**

The construction of plasmid pGLY-2 has been previously described (plasmid pHHD01K/ycdW-aceA-aceK (Martin et al., 2013)). Briefly, an artificial operon consisting of the genes *ycdW, aceA* and *aceK* (similar in structure to the endogenous *aceBAK* operon) was constructed and cloned into the multi-cloning site of pHHD01K (Martin et al., 2013) downstream of a Ptet promoter and ribosome binding site

between the EcoRI and BamHI sites. The vector allows polycistronic expression of the *ycdW-aceA-aceK* genes upon induction with anhydrotetracycline (aTc). pDHP-2a (pCDFDuet/pct/(acs-tesB)) was constructed by cloning an artificial operon consisting of the *acs* and *tesB* genes from *E. coli* into the NdeI and PacI sites of pCDFDuet/pct. For the construction of this operon, the genes *acs* and *tesB* were PCR amplified from MG1655 (DE3) gDNA template using the primer pairs NdeI-*acs*-FP + *acs*-RP and tesB-FP + PacI-*tesB*-RP (**Supplementary Table S1**) and were subsequently spliced together using SOEing PCR (Heckman and Pease, 2007; Horton et al., 1989).

Plasmids pETDuet-ΔT7 and pCDFDuet-ΔT7 were constructed by deleting the two regions containing the T7*lac* promoters, RBSs and multi-cloning sites from the parent plasmids pETDuet-1 and pCDFDuet-1, using primers listed in **Supplementary Table S1**. High fidelity Phusion Polymerase (Finnzymes, Espoo, Finland) was used for all PCR reactions to construct various fragments for cloning. MG1655 (DE3) gDNA template used for these reactions was isolated using the Wizard Genomic Purification Kit (Promega, Madison, WI).

The glycolate producing strains GP1, GP2, GP3 and GP4 (Table 1) were constructed via successively knocking out genes *iclR*, *aceB*, *gcl* and *glcB* from the parent strain MG1655 (DE3) (GP0) using P1 transduction to transfer knockout mutations from the corresponding Keio collection single knockout donor strains (Baba et al., 2006). Strain GP0-1 was constructed by transforming strain GP0 with the plasmid pGLY-1 to allow expression of *ycdW*, *aceA* and *aceK* upon induction with IPTG. Similarly, strains GP0-2, GP1-2 GP2-2, GP3-2 and GP4-2 were constructed by transforming GP0 to GP4 with the plasmid pGLY-2 which expresses the same enzymes upon induction with aTc. Positive transformants were isolated on LB agar plates supplemented with 50 mg/L of kanamycin. Strains GP0-1-DHP and GP0-2-DHP were created by co-transforming strains GP0-1 and GP0-2 with the 3,4-DHBA/3-HBL pathway plasmids pDHP-1 and pDHP-2, respectively, for integration of the glycolate and 3,4-DHBA/3HBL pathways and

positive transformants were selected on LB agar plates supplemented with 50 mg/L of ampicillin, 50 mg/L of streptomycin and 30 mg/L of kanamycin. Similarly, strains GP1-2-DHP to GP4-2-DHP were constructed by co-transforming pDHP-1 and pDHP-2 into strains GP1-2 to GP1-4. Strain GP0-1-EC was derived from GP0-1 by co-transforming with the empty Duet vectors pETDuet-1 and pCDFDuet-1, while the GP0-1-ΔT7C strain was obtained by co-transforming with the control vectors pETDuet-ΔT7 and pCDFDuet-ΔT7 lacking the T7*lac* promoter sites.

2.2. Culture conditions

Evaluation of glycolate, 3,4-DHBA and 3HBL synthesis by the various strains was performed in either 50 mL of Lysogeny Broth (LB) medium or M9 minimal salt medium (Sigma Aldrich) supplemented with varying amounts of glucose and appropriate antibiotics in 250 mL baffled shake flasks. The M9 salt medium cultures were additionally supplemented with 2 mM magnesium sulfate and 0.1 mM calcium chloride. Strains GP0-1 and GP0-2 were grown in media supplemented with kanamycin sulfate (50 mg/L), while strains GP0-1-DHP, GP0-2-DHP, GP0-1-EC, GP0-1-ΔT7 and GP1-2-DHP to GP4-2-DHP were cultured in media supplemented with ampicillin sulfate (50 mg/L), streptomycin sulfate (50 mg/L) and kanamycin sulfate (30 mg/L). For inoculation of the M9-glucose medium culture flasks, 5 mL seed cultures were grown overnight in LB (supplemented with appropriate antibiotics) at 37˚C and the centrifuged pellets were re-suspended in 1 ml of M9 minimal medium to minimize carryover of spent LB culture broth. These re-suspended cultures were used to inoculate 50 mL M9 minimal medium cultures supplemented with glucose to an initial OD_{600} of 0.1. The shake flask cultures were then incubated at 30°C on a rotary shaker at 250 rpm. LB cultures were inoculated directly with 2% (vol/vol) of an overnight LB seed culture. In both LB and M9 shake flask cultures, once the cells reached mid-exponential phase (when OD_{600} reached 0.8-1.0), pathway gene expression was induced by supplementing cultures with the appropriate inducers (250 ng/ml aTc and/or 100 µM or 1 mM IPTG). 1

mL of culture was withdrawn every 24 hours post-induction for up to 96 h to collect culture supernatants for HPLC analysis. Titers of various products reached a plateau by 72 h and there was essentially no difference in the titers between 72 h and 96 h; accordingly, only the peak titers observed at 72 h are reported. In general, experiments were performed in triplicates, and data are presented as the averages and standard deviations of the results.

2.3. Metabolite analysis using HPLC

Various metabolites were analyzed on an Agilent 1200 series HPLC instrument equipped with an Aminex HPX-87H ion exchange column (Biorad Laboratories, Hercules, CA) with 5 mM sulfuric acid as the mobile phase and a refractive index detector (RID). Standard curves were constructed using respective commercially available standards. A commercial standard was not available for 2,3-DHBA and 3HBL and these were quantified using the method described in Martin et al., 2013.

2.4. SDS-PAGE gel analysis of protein lysates

To prepare protein lysates, the respective *E. coli* strains were cultured in 50 ml of M9 minimal medium supplemented with 1% (wt/vol) glucose. The cultures were induced with IPTG (100 µM or 1 mM) in mid-exponential phase. Cell pellets prepared from 5 ml samples collected 6 hours post induction from each of the flasks were re-suspended in 1 mL of 10 mM Tris-HCl buffer (pH=8.0) containing 1 mg/mL lysozyme and were used to prepare crude lysates using cell disruption beads. Lysates were then clarified by centrifugation and separated electrophoretically into component proteins on 4-20% SDS-PAGE gels (BioRad Laboratories, Hercules, CA), loading about 15 µg of total protein into each well. Total protein levels in the crude lysates were measured using a modified Bradford assay (Zor and Seliger, 1996).

2.5. Quantification of mRNA transcript levels

The transcript levels for the mRNAs corresponding to *ycdW* and *aceA* were measured using a RT-qPCR assay. For this assay, the various strains were cultured in M9 minimal medium supplemented with 0.8% (wt/vol) glucose and were induced with 1 mM IPTG in mid-exponential phase. mRNA was isolated from cell samples (~10^9 cells) collected 6 hours post induction, using the illustra RNAspin Mini Kit (GE Healthcare Bio-Sciences, Piscataway, NJ). cDNA was synthesized via reverse transcription from each of the mRNA samples, with 500 ng of total RNA in each case, using the QuantiTect Reverse Transcription Kit (Qiagen, Valencia, CA) with random hexameric primers. *ycdW* and *aceA* mRNA levels were measured by amplifying the corresponding mRNAs from the synthesized cDNA in a qPCR reaction using the Brilliant II Sybr Green High ROX QPCR Mix (Agilent Technologies, Santa Clara, CA) on an ABI 7300 Real Time PCR instrument (Applied Biosystems, Beverly, CA), using *ycdW*-qPCR-FP and *ycdW*-qPCR-RP for the *ycdW* mRNA, and *aceA*-qPCR-FP and *aceA*-qPCR-RP primers for *aceA* mRNA, respectively (**Supplementary Table S1**). Transcript levels in each sample were measured in triplicate (three qPCR reactions each) with additional no-template and no-RT controls. Transcript levels for each of the mRNAs are reported relative to those for the same mRNA in strain GP0-1 (determined using a standard curve constructed using one of the strain GP0-1 samples), as averages of three flasks for each strain, each measured in triplicate.

3. Results

3.1. Investigating glycolate synthesis in *E. coli* with over-expression of pathway enzymes

Glycolate synthesis was initially investigated in the *E. coli* K-12 strain MG1655 (DE3) (strain GP0) transformed with pGLY-1 (strain GP0-1) that allows over-expression of the glycolate pathway enzymes YcdW, AceA and AceK from T7 promoters. Since part of the repression of the glyoxylate shunt during growth on glucose stems from transcriptional repression of expression of *aceA* and *aceK* from the *aceBAK* operon, over-expression of these genes is expected to relieve this repression and divert isocitrate flux towards glyoxylate. Experiments with GP0-1 were conducted in both LB and M9 minimal media supplemented with varying amounts of glucose. GP0-1 was observed to synthesize about 0.7 g/L of glycolate in M9 minimal medium cultures supplemented with 8 g/L glucose **(Figure 2a).** In comparison, GP0-1 cultures in the richer LB medium supplemented with glucose made considerably less glycolate with maximum titers of only 0.3 g/L, possibly due to repression of the glyoxylate shunt to a greater extent in the rich medium. Thus glucose supplemented M9 medium was selected for further studies.

3.2. Investigating integration of glycolate and 3,4-DHBA/3HBL pathways in glycolate producer GP0-1

We sought to integrate the glycolate and 3,4-DHBA/3HBL pathways in GP0-1 by co-transforming the 3,4-DHBA/3HBL pathway plasmids pDHP-1 and pDHP-2 to construct the strain GP0-1-DHP. No 3,4-DHBA or 3HBL synthesis was observed with GP0-1-DHP when cultured in M9 supplemented with various glucose (0.6 to 2%) concentrations at different induction levels (100 µM to 1 mM). The cultures were only observed to synthesize the pathway side product 3HB, formed due to the natural tendency of the 3,4-DHBA/3HBL pathway enzymes to condense two acetyl-CoA molecules, and the byproduct acetate (**Figure 2b**). Further, in comparison to GP0-1, GP0-1-DHP cultures produced less than 0.1 g/L of

glycolate indicating that the presence of the additional two 3,4-DHBA/3HBL pathway plasmids and expression of additional pathway enzymes had hampered glycolate synthesis in this strain.

To investigate this further, protein lysates were prepared from GP0-1 and GP0-1-DHP cultures for different levels of IPTG induction. As compared to lysates from wild-type and empty plasmid controls (**Supplementary Figure S3**), analysis on SDS-PAGE gels (**Figure 3a and b**) revealed that while GP0-1 over-expressed the glycolate pathway enzymes AceA and YcdW, similar over-expression of these enzymes was not observed in strain GP0-1-DHP. Instead, GP0-1-DHP only over-expressed the 3,4-DHBA/3HBL pathway enzymes Pct, BktB, PhaB and TesB. The negligible glycolate synthesis in GP0-1-DHP was thus attributed to insufficient expression of the glycolate pathway enzymes from pGLY-1 in the presence of the additional 3,4-DHBA/3HBL pathway plasmids. It should be noted that a band corresponding to AceK over-expression is not observed, even in lysates isolated from strain GP0-1, possibly due to the combined effect of transcriptional and translational control mechanisms that result in a 1000 fold lower expression of AceK in comparison to AceA (Cortay et al., 1989; Cozzone, 1998; Kornberg, 1966). However, in wild type *E. coli*, AceK is known to be highly active and present in a large excess over that required for its regulatory function (Stueland et al., 1989) and this lack of over-expression does not seem to affect glycolate synthesis adversely in GP0-1.

Various phenomena could be wholly or partially responsible for the observed reduced expression of the glycolate pathway enzymes in the presence of additional pathway plasmids, including: a) plasmid loss or instability, b) transcriptional limitations resulting in reduced mRNA levels due to reduced T7 RNA polymerase (RNAP) availability, c) differences in mRNA stability affecting mRNA levels, and d) translational limitations due to competition for ribosomal machinery amongst different mRNAs. Restriction digests of plasmids isolated from the cultures 6 hours post induction showed that all plasmids were retained as expected by the GP0-1-DHP cells, and the plasmid copy number of pGLY-1 was not reduced relative to GP0-1 (**Supplementary Figure S4**). The relative copy numbers of the three

plasmids in GP0-1-DHP was found to be pDHP-1>pDHP-2>pGLY-1, consistent with the replicons of the vectors. Translational limitations are only expected to be a significant cause of the observed expression loss if mRNA levels of the target transcripts have not been substantially reduced. Thus, we directed additional experiments towards measuring mRNA transcript levels to further investigate if transcriptional limitations arising out of T7 RNAP availability and/or mRNA stability were responsible for the hampered expression.

3.3. Investigating transcriptional limitations due to reduced T7 RNAP availability

Integration of the pathways in GP0-1-DHP relies on the simultaneous over-expression of all 7 pathway enzymes from their respective genes cloned downstream of T7*lac* promoters and ribosome binding sites in the three Duet vector derived plasmids pDHP-1, pDHP-2 and pGLY-1. All three pathway plasmids depend on T7 RNAP to initiate transcription of the pathway genes, which is synthesized in each of the strains from the chromosomally integrated DE3 prophage cassette upon induction with IPTG. While all of the T7 RNAP synthesized in the GP0-1 cells is exclusively available to initiate expression of the glycolate pathway enzymes via transcription from multiple copies of pGLY-1, the same T7 RNAP in GP0-1-DHP is distributed between multiple copies of the three different plasmids (pDHP-1, pDHP-2 and pGLY-1), reducing the amount of T7 RNAP available to initiate transcription from each copy of the three different plasmids. We hypothesized that in GP0-1-DHP, this reduced T7 RNAP availability in the presence of the additional pDHP-1 and pDHP-2 plasmids was hampering the expression of the glycolate pathway enzymes from the lower copy pGLY-1 plasmid, preventing effective glycolate synthesis.

To test this hypothesis, glycolate synthesis and glycolate pathway enzyme transcript levels were measured and compared in strains GP0-1, GP0-1-ΔT7, GP0-1-EC and GP0-1-DHP. Similar to T7 RNAP sequestration by pDHP-1 and pDHP-2 in GP0-1-DHP, the T7*lac* promoter sites in the empty plasmids are expected to sequester some of the available T7 RNAP away from pGLY-1 in GP0-1-EC, though to a lesser extent due to lack of active sustained transcription, while also imposing a slightly decreased burden due

to the inability to actually express any recombinant protein and smaller sizes of the empty plasmid vectors. Indeed, GP0-1-EC was observed to have produced less glycolate than GP0-1 but more than GP0-1-DHP (**Figure 4a**). On the other hand, deletion of the T7 promoter sites in pETDuet-ΔT7 and pCDFDuet-ΔT7 is expected to alleviate the T7 RNAP sequestration problem. GP0-1-ΔT7 was observed to produce more glycolate than GP0-1-EC, though to a lesser extent than GP0-1, possibly due to the burden of maintaining the additional pETDuet-ΔT7 and pCDFDuet-ΔT7 plasmids (**Figure 4a**).

The transcript levels for the *ycdW* and *aceA* mRNAs in these strains were then measured and compared (**Figure 4b and c**). The mRNA transcript levels for both *ycdW* and *aceA* in strains GP0-1-EC and GP0-1-DHP are several fold lower than the corresponding GP0-1 and GP0-1-ΔT7 transcript levels. In particular, for strain GP0-1-DHP, the *ycdW* transcript levels were 80-fold lower while the *aceA* transcript levels were 36-fold lower than those observed with GP0-1. Thus, the reduced transcript levels may be in part attributed to T7 RNAP sequestration by pDHP-1 and pDHP-2 and result in poor expression of *ycdW* and *aceA* and negligible glycolate synthesis in GP0-1-DHP.

3.4. Alleviating T7 RNAP limitations through the use of an orthogonal expression system

To alleviate the T7 RNAP limitation, we employed an orthogonal expression system that allows expression of the glycolate pathway enzymes independent of T7 RNAP. The glycolate pathway genes *ycdW*, *aceA* and *aceK* were cloned as an operon into pHHD01K, downstream of an aTc inducible Ptet promoter and ribosome binding site to construct pGLY-2. Strain GP0-2 carrying pGLY-2 cultured in minimal medium supplemented with glucose upon induction with aTc resulted in glycolate synthesis superior to GP0-1 with titers of up to 1455 ± 209 mg/L. The initial glucose concentration (**Supplementary Figure S5**) as well as the aTc concentration (data not shown) used for induction were observed to have a negligible effect on glycolate synthesis with GP0-2. Similar to GP0-1, strain GP0-2 was observed to synthesize glycolate to a much lesser extent in LB, with maximum titers of only about 0.5 g/L. Additionally, GP0-2-DHP carrying this new glycolate pathway plasmid in addition to pDHP-1 and

pDHP-2 cultured in M9-glucose medium synthesized up to 1280 ± 41 mg/L of glycolate. Protein lysates from GP0-2-DHP showed the expected over-expression of the glycolate pathway enzymes in addition to the DHBA/3HBL pathway enzymes (**Supplementary Figure S6**). Further, we observed direct synthesis of up to 699 ± 109 mg/L of 3,4-DHBA and 312 ± 12 mg/L of 3HBL from glucose as a sole carbon source in this integrated system alongside 317 ± 9 mg/L of 3HB and 633 ± 62 mg/L of 2,3-DHBA as side products. While the overall titers for 3,4-DHBA and 3HBL obtained by such direct synthesis from glucose are lower than those obtained with exogenous glycolate feeding, they represent about 24.2% of the maximum theoretical pathway yield (**Supplementary Table S2**). Interestingly, direct synthesis from glucose resulted in a slightly higher selectivity ratio of 3,4-DHBA + 3HBL to the 2,3-DHBA isomer in comparison to exogenous glycolate feeding (**Supplementary Figure S1** and **Supplementary Table S2**).

3.5. Carbon utilization, product distribution and strain engineering

The use of two orthogonal expression systems also allowed us to exercise independent control over the expression of the glycolate and DHBA/3HBL pathway enzymes and the distribution of carbon flux between glycolate synthesis and the synthesis of 3-hydroxyacid pathway products (**Figure 5a and b**). For a given aTc inducer concentration, increasing the level of IPTG induction from 50 to 100 μM is expected to increase the expression levels for the downstream pathway enzymes and resulted in an increase in the titers of the total hydroxyacid products (DHBA+3HBL+3HB). Interestingly, this increase in the hydroxyacid products was accompanied by an increase in the net glycolate synthesized, suggesting that consumption of glycolate along the downstream pathway promoted more glycolate synthesis upstream. However, further increasing the IPTG induction level to 200 μM resulted in reduced hydroxyacid production as well as reduced net glycolate synthesis, suggesting metabolic stress. The highest total DHBA + 3HBL titers (about 10.5 mM) were observed at 250 ng/ml aTc and 100 μM IPTG inducer concentrations.

We also investigated the effect of varying the supplied glucose substrate concentration on the product profile. The titers for 3,4-DHBA and 3HBL were observed to double with an increase in the glucose supplementation from 8 g/L to 10 g/L (**Figure 6a** and **Supplementary Table S3**), with a negligible influence of a further increase to 15 g/L. As observed from **Figure 6b**, for different starting glucose concentrations, the cells utilized roughly 5 g/L of the supplied glucose for building biomass and for maintenance functions and the balance was available for conversion to desired products and unwanted by-products. In the case of 8 g/L of supplied glucose, a large fraction of the remaining 3 g/L glucose was observed to be converted to glycolate with only a small amount converted to the final products of interest (DHBA and 3HBL). This is suggestive of glucose exhaustion before the synthesized glycolate may be converted substantially along the downstream pathway to DHBA and 3HBL. When the supplied glucose concentration was increased to 10 g/L, the biocatalyst not only synthesized glycolate, but also converted it into DHBA and 3HBL using the additional available glucose, resulting in a two-fold increase in the titers of DHBA and 3HBL and corresponding decrease in titers for glycolate. However, the cells showed a limited capacity to process supplied carbon, and further increasing the supplied glucose concentration to 15 g/L did not result in higher titers, with about 5 g/L of glucose left unconsumed. The underlying reasons for the inability to completely consume the supplied glucose are currently under investigation in our lab and include such conditions as unfavorable pH, biocatalyst inactivation, and product inhibition. We do note that production of the organic acids glycolate and DHBA does result in a significant reduction in the pH of these cultures, which we have previously found to limit synthesis of other organic acids (Shiue and Prather, 2014).

We investigated the overexpression of the endogenous acetyl-CoA synthetase gene (*acs*) from *E. coli* in the strain DHP0 to recycle the acetate formed as a result of the activation of glycolate by Pct. DHBA and 3HBL synthesis from exogenously fed glycolate in LB was compared with and without Acs overexpression in strains DHP0+*acs* and DHP0, respectively. While the acetate titers with Acs expression

were lower than those without (suggesting some degree of acetate recycling), these did not translate to higher 3HB or DHBA/3HBL titers (**Supplementary Figure S7**). In fact, the expression of Acs seemed to hamper both the total DHBA + 3HBL and 3HB titers, suggesting a metabolic burden, either due to its expression or due to the consumption of ATP by Acs in the activation reaction. Similar results were obtained with Acs over-expression in the case of DHBA/3HBL synthesis from endogenously synthesized glycolate in strain GP0-2-DHP+*acs* in M9-glucose medium.

We also investigated glycolate, DHBA and 3HBL synthesis with *ycdW*, *aceA* and *aceK* over-expression in strains engineered to eliminate different endogenous glycolate and glyoxylate consumption pathways (strains GP1, GP2, GP3 and GP4). This approach had previously resulted in improved glycolate synthesis when used in combination with over-expression of *ycdW* alone (Soucaille, 2009). However, none of the engineered strains showed appreciably improved glycolate or DHBA/3HBL synthesis at the shake flask scale (**Supplementary Figure S8a and b**), suggesting that over-expression of *ycdW*, *aceA* and *aceK* alone allows sufficient glycolate synthesis in the base strain GP0 at the shake flask scale. These preliminary observations warrant a more detailed study of these and other engineered strains at the bioreactor scale.

4. Discussion

The direct synthesis of 3,4-DHBA and 3HBL from glucose as a sole carbon source via integration of the *de novo* constructed 3HA pathway with the endogenous glyoxylate shunt represents a promising opportunity for the stereospecific biosynthesis of these valuable chemicals from inexpensive simple sugars. The pathway affords a maximum theoretical pathway yield Y^P (Dugar and Stephanopoulos, 2011) of 0.66 mole/mole of glucose which may be increased to 1 mole/mole by recycling acetate that is formed as a by-product. While this is lower than the absolute pathway independent maximum yield, Y^E of 1.5 moles/mole on glucose as a substrate (**see Supplementary Calculations**), to the best of our knowledge, to date, there aren't known processes or catalysts that allow such an efficient conversion of an inexpensive sugar like glucose to 3HBL or 3,4-DHBA in a stereospecific manner. This first demonstration of biosynthesis of up to 24.2% of this theoretical pathway maximum with a close to wild type *E. coli* K-12 strain at the shake flask scale, while promising, warrants further improvement.

We foresee enhancing pathway yield using two possible levers: a) improving pathway selectivity through the screening of alternative pathway enzymes and b) reducing loss of carbon towards excess biomass and unwanted products via host and fermentation engineering. The condensation reaction between glycolyl-CoA and acetyl-CoA is the first step that commits carbon flux towards 3,4-DHBA and 3HBL. BktB and other natural thiolases exhibit a natural activity towards synthesis of 3HB and 2,3-DHBA as inevitable major side products, with roughly 1 mole of 3HB + 2,3-DHBA synthesized per mole of 3,4-DHBA + 3-HBL (**Supplementary Table S2**). Screening or possibly engineering of a suitable thiolase enzyme with higher activity and selectivity towards the synthesis of the 3,4-DHBA precursor condensation product and reduced formation of 3HB or 2,3-DHBA can help enhance titers to approach the theoretical pathway yield. The observation that this selectivity ratio improved slightly with endogenous glycolate synthesis in comparison to exogenous glycolate feeding, possibly due to

differences in the relative intracellular levels of glycolyl-CoA and acetyl-CoA, suggests the potential to use specific glucose feeding and fermentation strategies to manipulate these pools to improve yield.

Part of the loss in theoretical pathway yield may be attributed to the generation of acetate as a by-product of the activation reaction of glycolate to glycolyl-CoA by Pct. Recycling this acetate to acetyl-CoA using Acs may allow us to boost the yield. Indeed, eliminating acetate as a by-product by incorporating this recycle reaction in the theoretical pathway yield calculation increases Y^P to 1 mole/mole of glucose. While recycling this acetate as acetyl-CoA comes at the expense of consumption of energy (in the form of ATP), the pathway produces an excess of energy rich reducing equivalents and this additional ATP consumption is in theory not expected to impose an unfavorable additional burden. However, our preliminary results suggest that over-expression of acetyl-CoA synthetase does in fact impose a burden (**Supplementary Figure S7**), affecting product titers. Moving forward, a finer tuning of this over-expression may be required.

In this study, the use of two orthogonal expression systems to independently express the two sets of pathway enzymes was critical for the successful over-expression of all pathway proteins. The extent of protein over-expression from an inducible plasmid is dependent upon many factors, including plasmid copy number, induction level, mRNA stability, and efficiency of transcription and translation, amongst others. This expression is expected to be limited by mRNA levels and stability at low transcript levels arising from lower levels of induction and/or low plasmid copy numbers (Carrier et al., 1998), and translation and ribosomal machinery limited at higher transcript levels resulting from higher induction levels and/or copy numbers (Birnbaum and Bailey, 1991). In the present system, we observed an mRNA limitation arising from reduced transcription due to T7 RNAP sequestration. At the same time, we cannot rule out the possibility of an additional translational limitation which would depend on the total collective transcript levels for all over-expressed proteins and the relative translation initiation rates. The T7 RNAP sequestration problem uncovered in this study may similarly impede expression from

multiple T7 promoters and affect product synthesis in other pathways. The extent and gravity of this effect is expected to be context dependent and influenced by multiple factors including overall metabolic burden, stability of mRNA transcripts, efficiency of translation of generated transcripts, catalytic efficiency (activity) of individual enzymes with their respective substrates and the required (optimal) level of over-expression for each enzyme. Indeed, in other pathways in our laboratory, we have effectively achieved simultaneous expression of multiple enzymes from up to 4 different Duet vectors with 8 different T7 promoter sites (Tseng and Prather, 2012). Nevertheless, this highlights the need for well-characterized orthogonal parts (such as promoters, RBSs etc.) and expression systems that can allow one to readily vary expression levels of multiple different pathway enzymes in the *de novo* construction of metabolic pathways.

5. Conclusions

We have established the first complete biosynthetic pathway for the direct synthesis of 3HBL from glucose as a sole feedstock in a close to wild type *E. coli* strain, synthesizing up to 0.70 g/L of the free acid 3,4-DHBA and 0.31 g/L of 3HBL. In the course of our initial attempts at assembling and integrating the glycolate and 3,4-DHBA/3HBL synthesis pathway, we uncovered T7 RNA polymerase sequestration as a potential limitation that may impede expression of multiple pathway enzymes using multiple Duet vectors under metabolically stressful conditions. Distribution of pathway enzymes between orthogonal expression systems such as the ones employed in our pathway can serve to effectively alleviate this problem and afford reliable expression of multiple pathway enzymes. Using the integrated pathway, we have been successful in achieving up to 24.2% of the theoretical yield with potential for further enhancing pathway performance through the various approaches discussed. Finally, this preliminary demonstration of direct synthesis from glucose now opens avenues towards the synthesis of 3HBL and

3,4-DHBA as value-added, biomass-derived biochemicals from other simple sugars that are products of breakdown of biomass.

Acknowledgements

This work was supported by the National Science Foundation through the Synthetic Biology Engineering Research Center (SynBERC, Grant No. EEC-0540879).

Conflict of Interest

HD, CHM and KLJP declare conflict of interests due to issued and outstanding patent applications covering aspects of this work.

References

Baba, T., Ara, T., Hasegawa, M., Takai, Y., Okumura, Y., Baba, M., Datsenko, K. A., Tomita, M., Wanner, B. L., Mori, H., 2006. Construction of Escherichia coli K-12 in-frame, single-gene knockout mutants: the Keio collection. Mol Syst Biol. 2.

Birnbaum, S., Bailey, J. E., 1991. Plasmid presence changes the relative levels of many host-cell proteins and ribosome components in recombinant *Escherichia coli*. Biotechnology And Bioengineering. 37**,** 736-745.

Byun, I. S., Kim, K. I., Bong, C. A., Process for the preparation of L-carnitine. In: Office, U. S. P., (Ed.). Samsung Fine Chemicals Company Ltd., KR, United States, 2002.

Carrier, T., Jones, K. L., Keasling, J. D., 1998. mRNA stability and plasmid copy number effects on gene expression from an inducible promoter system. Biotechnology And Bioengineering. 59**,** 666-672.

Cortay, J. C., Bleicher, F., Duclos, B., Cenatiempo, Y., Gautier, C., Prato, J. L., Cozzone, A. J., 1989. Utilization of acetate in Escherichia coli - Structural organization and differential expression of the ace operon. Biochimie. 71**,** 1043-1049.

Cozzone, A. J., 1998. Regulation of acetate metabolism by protein phosphorylation in enteric bacteria. Annual Review Of Microbiology. 52**,** 127-164.

Dugar, D., Stephanopoulos, G., 2011. Relative potential of biosynthetic pathways for biofuels and bio-based products. Nature Biotechnology. 29**,** 1074-1078.

Furrow, M. E., Schaus, S. E., Jacobsen, E. N., 1998. Practical access to highly enantioenriched C-3 building blocks via hydrolytic kinetic resolution. Journal Of Organic Chemistry. 63**,** 6776-6777.

Heckman, K. L., Pease, L. R., 2007. Gene splicing and mutagenesis by PCR-driven overlap extension. Nat. Protocols. 2**,** 924.

Horton, R. M., Hunt, H. D., Ho, S. N., Pullen, J. K., Pease, L. R., 1989. Engineering Hybrid Genes Without The Use Of Restriction Enzymes - Gene-Splicing By Overlap Extension. Gene. 77**,** 61-68.

Hwang, J. Y., Park, J., Seo, J. H., Cha, M., Cho, B. K., Kim, J., Kim, B. G., 2009. Simultaneous Synthesis of 2-Phenylethanol and L-Homophenylalanine Using Aromatic Transaminase With Yeast Ehrlich Pathway. Biotechnology And Bioengineering. 102**,** 1323-1329.

Kornberg, H. L., 1966. Role and control of glyoxylate cyncle in Escherichia coli Biochemical Journal. 99**,** 1-12.

Kumar, P., Deshmukh, A. N., Upadhyay, R. K., Gurjar, M. K., 2005. A simple and practical approach to enantiomerically pure (S)-3-hydroxy-γ-butyrolactone: synthesis of (R)-4-cyano-3-hydroxybutyric acid ethyl ester. Tetrahedron: Asymmetry. 16**,** 2717-2721.

Laporte, D. C., Koshland, D. E., 1982. A protein with kinase and phosphatase activities involved in regulation of tricarboxylic acid cycle. Nature. 300**,** 458-460.

Lee, S. H., Park, O. J., 2009. Uses and production of chiral 3-hydroxy-gamma-butyrolactones and structurally related chemicals. Applied Microbiology And Biotechnology. 84**,** 817-828.

Martin, C. H., Dhamankar, H., Tseng, H.-C., Sheppard, M. J., Reisch, C. R., Prather, K. L. J., 2013. A platform pathway for production of 3-hydroxyacids provides a biosynthetic route to 3-hydroxy-gamma-butyrolactone. Nature Communications. 4**,** 1-7.

Masamune, S., Palmer, M. A. J., Gamboni, R., Thompson, S., Davis, J. T., Williams, S. F., Peoples, O. P., Sinskey, A. J., Walsh, C. T., 1989. Bio-Claisen condensation catalyzed by thiolase from Zoogloea ramigera. Active site cysteine residues. J. Am. Chem. Soc. 111**,** 1879.

Nakagawa, A., Idogaki, H., Kato, K., Shinmyo, A., Suzuki, T., 2006. Improvement on production of (R)-4-Chloro-3-hydroxybutyrate and (S)-3-hydroxy-gamma-butyrolactone with recombinant Escherichia coli cells. Journal Of Bioscience And Bioengineering. 101**,** 97-103.

Nimmo, G. A., Nimmo, H. G., 1984. The regulatory properties of isocitrate dehydrogenase kinase and isocitrate dehydrogenase phosphatase from Escherichia coli ML308 and the roles of these activities in the control of isocitrate dehydrogenase. European Journal of Biochemistry. 141**,** 409-414.

Park, Y. M., Chun, J. P., Rho, K. R., Yu, H. S., Hwang, I., Process for preparing optically pure (S)-3-hydroxy-γ-butyrolactone. In: Office, U. S. P., (Ed.), United States Patent Application Publication. Samsung Fine Chemicals Co., Ltd., United States, 2004.

Shin, H. I., Chang, J. H., Woo, Y. M., Yim, Y. S., A process for the synthesis of 3-hydroxy-γ-butyrolactone. In: Organization, W. I. P., (Ed.). LG Life Science Ltd., United States, 2005.

Shiue, E., Prather, K. L. J., 2014. Improving D-glucaric acid production from myo-inositol in E. coli by increasing MIOX stability and myo-inositol transport. Metabolic Engineering. 22**,** 22-31.

Soucaille, P., Glycolic acid production by fermentation from renewable resources. In: Office, U. S. P., (Ed.), United States, 2009.

Stueland, C. S., Ikeda, T. P., Laporte, D. C., 1989. Mutation of the predicted ATP binding-site inactivates both activities of isocitrate dehydrogenase kinase phosphatase Journal Of Biological Chemistry. 264**,** 13775-13779.

Suzuki, T., Idogaki, H., Kasai, N., 1999. Dual production of highly pure methyl (R)-4-chloro-3-hydroxybutyrate and (S)-3-hydroxy-gamma-butyrolactone with Enterobacter sp. Enzyme And Microbial Technology. 24**,** 13-20.

Tseng, H. C., Martin, C. H., Nielsen, D. R., Prather, K. L., 2009. Metabolic engineering of Escherichia coli for enhanced production of (R)- and (S)-3-hydroxybutyrate. Appl Environ Microbiol. 75**,** 3137 - 3145.

Tseng, H. C., Prather, K. L. J., 2012. Controlled biosynthesis of odd-chain fuels and chemicals via engineered modular metabolic pathways. Proceedings Of The National Academy Of Sciences Of The United States Of America. 109**,** 17925-17930.

Wang, G. J., Hollingsworth, R. I., 1999. Direct conversion of (S)-3-hydroxy-gamma-butyrolactone to chiral three-carbon building blocks. Journal Of Organic Chemistry. 64**,** 1036-1038.

Werpy, T., Peterson, G., 2004. Top value added chemicals from biomass, Vol 1: results of screening for potential candidates from sugars and synthesis gas.

Yang, H., Goyal, N., Ella-Menye, J. R., Williams, K., Wang, G. J., 2012. Synthesis of Chiral Five-, Six-, and Seven-Membered Heterocycles from (S)-3-Hydroxy-gamma-butyrolactone. Synthesis-Stuttgart. 44**,** 561-568.

Zor, T., Seliger, Z., 1996. Linearization of the bradford protein assay increases its sensitivity: Theoretical and experimental studies. Analytical Biochemistry. 236**,** 302-308.

1

Table 1 | *E. coli* strains and plasmids

Name	Relevant Genotype	Reference
Strains		
DH10B	F$^-$ *mcr*A Δ(*mrr-hsd*RMS-*mcr*BC) ϕ80*lac*ZΔM15 Δ*lacX74 recA1 endA1 araD139*Δ(*ara, leu*)7697 *galU galK* λ$^-$ *rpsL nupG*	Invitrogen
ElectroTen-Blue	Δ(*mcrA*)*183* Δ*(mcrCB-hsdSMR-mrr)173 endA1 supE44 thi-1 recA1 gyrA96 relA1 lac* Kan^r [F′ *proAB lacI*^{q}ZΔM15 Tn*10* (Tet^r)]	Stratagene
MG1655 (DE3)	F$^-$ λ$^-$ *ilvG- rfb-50 rph-1 with the DE3 prophage integrated*	Tseng 2010
DHP0	MG1655 (DE3) carrying pDHP-1 and pDHP-2	This study
DHP0+*acs*	MG1655 (DE3) carrying pDHP-1 and pDHP-2a	This study
GP0-1	MG1655 (DE3) carrying pGLY-1	This study
GP0-1-DHP	GP0-1 containing pDHP-1 and pDHP-2	This study
GP0-2	MG1655(DE3) carrying pGLY2	This study
GP0-2-DHP	GP0-2 carrying pDHP-1 and pDHP-2	This study
GP0-2-DHP+*acs*	GP0-2 carrying pDHP-1 and pDHP-2a	This study
GP1	MG1655 (DE3) Δ*iclR*	This study
GP2	MG1655 (DE3) Δ*iclR,* Δ*aceB*	This study
GP3	MG1655 (DE3) Δ*iclR,* Δ*aceB,* Δ*gcl*	This study
GP4	MG1655 (DE3) Δ*iclR,* Δ*aceB,* Δ*gcl,* Δ*glcB*	This study
GP1-2	GP1 carrying pGLY-2	This study
GP2-2	GP2 carrying pGLY-2	This study
GP3-2	GP3 carrying pGLY-2	This study
GP4-2	GP4 carrying pGLY-2	This study
GP1-2-DHP	GP1-2 carrying pDHP-1 and pDHP-2	This study
GP2-2-DHP	GP2-2 carrying pDHP-1 and pDHP-2	This study
GP3-2-DHP	GP3-2 carrying pDHP-1 and pDHP-2	This study
GP4-2-DHP	GP4-2 carrying pDHP-1 and pDHP-2	This study
Plasmids		
pETDuet-1	ColE1(pBR322) *ori*, *lacI,* T7*lac*, Amp^R	Novagen
pCDFDuet-1	CloDF13 *ori*, *lacI,* T7*lac*, Strep^R	Novagen
pCOLADuet-1	ColA *ori*, *lacI,* T7*lac*, Kan^R	Novagen
pHHD01K	p15 *ori, tetR,* Ptet, Kan^R	This study
pGLY-1	pCOLADuet-1 harboring *ycdW* and *aceA-aceK* from *E.coli* MG1655	This study
pGLY-2	pHHD01K harboring the genes *ycdW, aceA and aceK* from *E.coli* MG1655 in an artificial operon similar in structure to the *aceBAK* operon	This study

pDHP-1	pETDuet-1 harboring *bktB* and *phaB* from *C.necator* named pET/bktB/phaB in Martin *et al*, 2013	Martin et al, 2013
pDHP-2	pCDFDuet-1 harboring *pct* from *M. elsdenii*, and *tes*B from *E. coli* MG1655 named pCDF/pct/tesB in Martin *et al*, 2013	Martin et al, 2013
pDHP-2a	pCDFDuet-1 harboring *pct* from *M. elsdenii*, and an artificial operon of the genes *acs and tes*B from *E. coli* MG1655	This study

1

2

Figure Legends

Figure 1 | DHBA and 3-HBL synthesis pathway. Expression of *pct*, *bktB*, *phaB* and *tesB* in *E. coli* allows DHBA and 3HBL synthesis from glucose and glycolic acid. Pct activates glycolic acid to glycolyl-CoA. BktB brings about the condensation of glycolyl-CoA with acetyl-CoA (from glycolysis) to form 4-hydroxy-3-ketobutyryl-CoA, which is reduced by PhaB to *(S)*-3,4-dihydroxybutyryl-CoA. TesB cleaves CoA from *(S)*-3,4-dihydroxybutyryl-CoA to form *(S)*-3,4-DHBA while a part of the *(S)*-3,4-dihydroxybutyryl-CoA spontaneously lactonizes to *(S)*-3HBL. An alternative condensation reaction between glycolyl-CoA and acetyl-CoA results in the 2,3-DHBA isomer, while a condensation between two acetyl-CoAs results in 3-hydroxybutyrate (3HB).

Figure 2 | Product synthesis by strains GP0-1 and GP0-1-DHP. a) Glycolate titers for GP0-1 cells cultured in LB or M9 media supplemented with 8, 10 or 15 g/L glucose b) Titers for different products synthesized by strain GP0-1-DHP cultured in M9 minimal medium supplemented with 8 or 10 g/L glucose. All cultures were induced with 1 mM IPTG and titers are reported 72 hours post induction. Data are presented as the mean ± s.d. (n=3).

Figure 3 | Expression of pathway enzymes in recombinant strains GP0-1 and GP0-1-DHP. Protein lysates isolated from strains GP0-1 and GP0-1-DHP, grown in minimal medium supplemented with 1% glucose and induced with a) 100 µM IPTG and b) 1 mM IPTG were loaded on a SDS-PAGE gel for separation. For each gel, lanes 1-3 on the left show lysates from GP0-1 cultures (3 replicates) while 5-7 show lysates from GP0-1-DHP. Lane 4 was loaded with the unstained protein ladder. Similar results were observed for cultures induced with 500 µM IPTG. Expected sizes of proteins: PhaB = 26.7 kD, TesB = 31.9 kD, YcdW = 35.4 kD, BktB = 40.9 kD, AceA = 47.5 kD, Pct = 56.0 kD and AceK = 67.7 kD.

Figure 4 | Glycolate synthesis in engineered strains. All strains were cultured in M9 medium supplemented with 0.8% glucose at 30 ˚C with 1 mM IPTG induction in triplicate. a) Glycolate titers reported as mean ± s.d. (n=3). b) *ycdW* mRNA transcript levels and c) *aceA* mRNA transcript levels, quantified relative to the corresponding transcript levels in strain GP0-1 using a standard curve, reported as mean ± s.d. (n=3).
Strains: 1) GP0-1 = MG1655 (DE3) + pGLY-1, 2) GP0-1-ΔT7 = GP0-1 carrying pETDuet-ΔT7 and pCDFDuet-ΔT7, 3) GP0-1-EC = GP0-1 carrying pETDuet and pCDFDuet and 4) GP0-1-DHP = GP0-1 carrying pDHP-1 and pDHP-2.

Figure 5 | Effect of varying inducer levels on DHBA synthesis. a) Total DHBA (both isomers) + 3HBL titers in mM for GP0-2-DHP cultured in M9 medium supplemented with 1% glucose for different induction levels. b) Total hydroxyacid (HA) product titers are the sum of the titers for the two DHBA isomers, 3HBL and 3HB. Net glycolate synthesized is calculated as the sum of the glycolate titers at the end of 72 hours and the glycolate that ends up as DHBA + 3HBL (based on the t=72 h titers for the two DHBA isomers and 3HBL). The x-axis in the plot denotes different inducer combinations (e.g.: 50A-50I denotes induction with 50 ng/ml aTc (A) and 50 µM IPTG (I) and so on).

Figure 6 | Product profiles and distribution of carbon in the synthesis of glycolate, DHBA and 3HBL with GP0-2-DHP. GP0-2-DHP was cultured in M9 minimal medium supplemented with varying amounts of glucose (8, 10 and 15 g/L), induced with aTc (250 ng/ml) and IPTG (100 µM). a) Product titers, 72 hours post induction and b) Distribution of supplied glucose between different products. The amount of glucose consumed for the synthesis of each of the products is estimated from the corresponding final product titer (**Supplementary Table S3 and S4b**), using the theoretical reaction for synthesis of each product as listed in the **Supplementary Calculations**. All flask cultures were run in triplicate with product titers reported as mean ±s.d. (n=3).

Figure 1

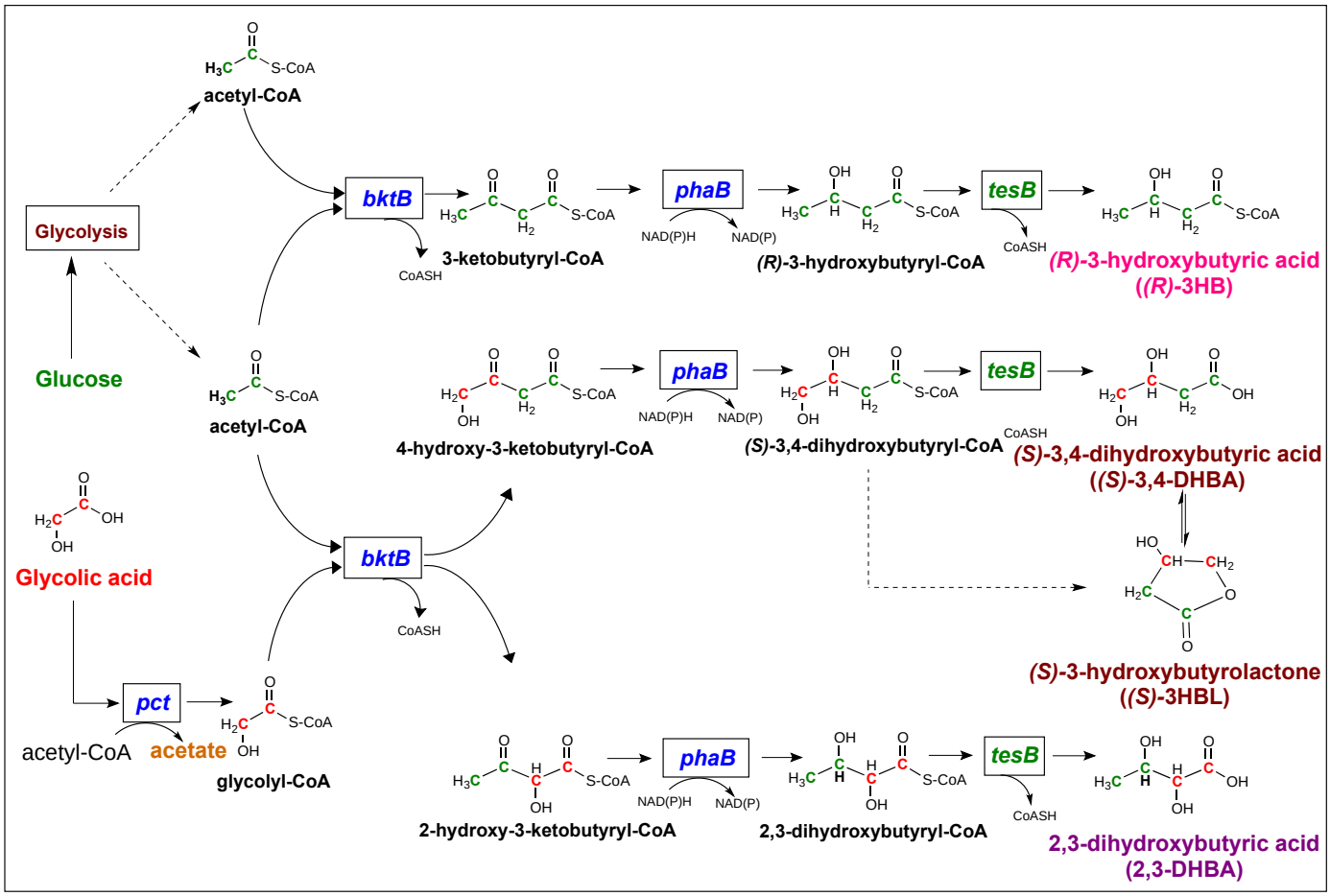
acetyl-CoA
Glycolysis
bktB
3-ketobutyryl-CoA
CoASH
phaB
NAD(P)H
NAD(P)
(R)-3-hydroxybutyryl-CoA
tesB
CoASH
(R)-3-hydroxybutyric acid
((R)-3HB)
Glucose
acetyl-CoA
4-hydroxy-3-ketobutyryl-CoA
(S)-3,4-dihydroxybutyryl-CoA
(S)-3,4-dihydroxybutyric acid
((S)-3,4-DHBA)
Glycolic acid
bktB
CoASH
(S)-3-hydroxybutyrolactone
((S)-3HBL)
pct
acetyl-CoA
acetate
glycolyl-CoA
2-hydroxy-3-ketobutyryl-CoA
2,3-dihydroxybutyryl-CoA
2,3-dihydroxybutyric acid
(2,3-DHBA)

Figure 2

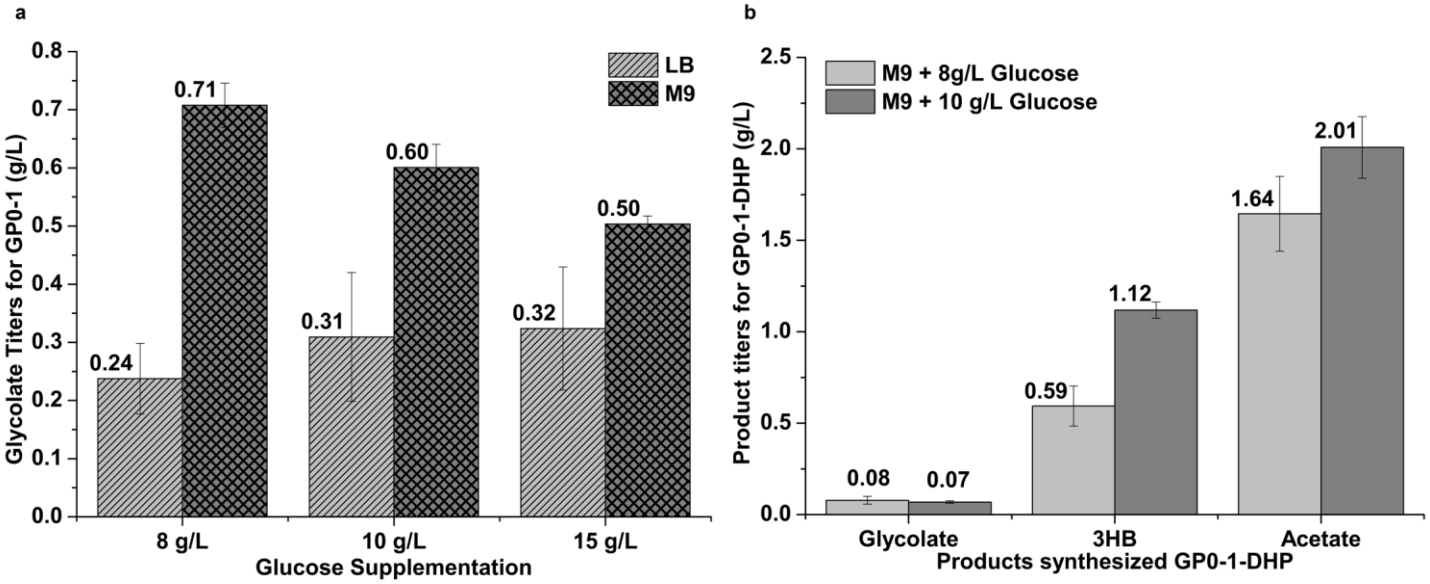
a
Glycolate Titers for GP0-1 (g/L)
0.0
0.1
0.2
0.3
0.4
0.5
0.6
0.7
0.8
LB
M9
0.24
0.71
0.31
0.60
0.32
0.50
8 g/L
10 g/L
15 g/L
Glucose Supplementation
b
Product titers for GP0-1-DHP (g/L)
0.0
0.5
1.0
1.5
2.0
2.5
M9 + 8g/L Glucose
M9 + 10 g/L Glucose
0.08
0.07
0.59
1.12
1.64
2.01
Glycolate
3HB
Acetate
Products synthesized GP0-1-DHP

Figure 3

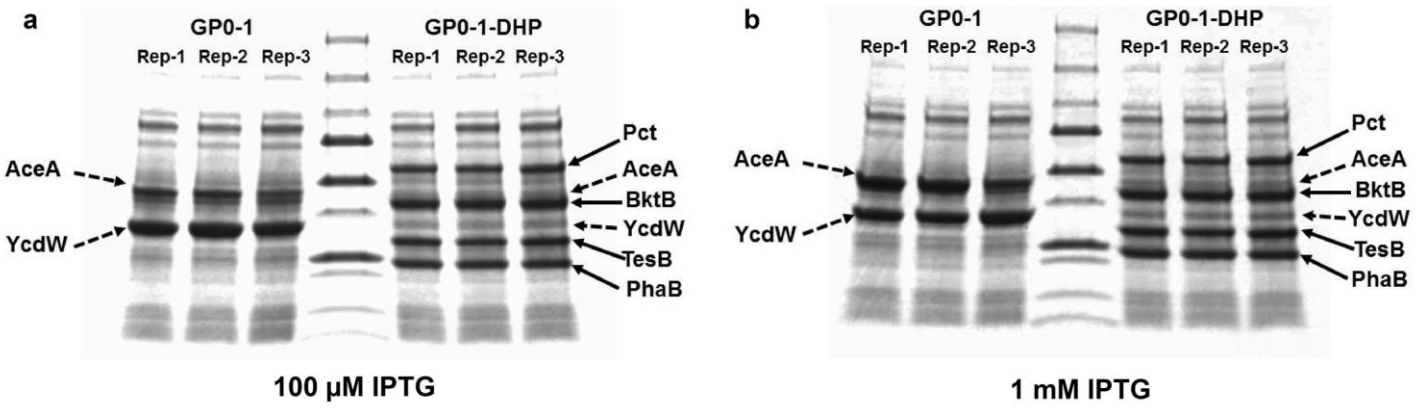
a
GP0-1
GP0-1-DHP
Rep-1 Rep-2 Rep-3
Rep-1 Rep-2 Rep-3
AceA
YcdW
Pct
AceA
BktB
YcdW
TesB
PhaB
100 µM IPTG
b
GP0-1
GP0-1-DHP
Rep-1 Rep-2 Rep-3
Rep-1 Rep-2 Rep-3
AceA
YcdW
Pct
AceA
BktB
YcdW
TesB
PhaB
1 mM IPTG

Figure 4

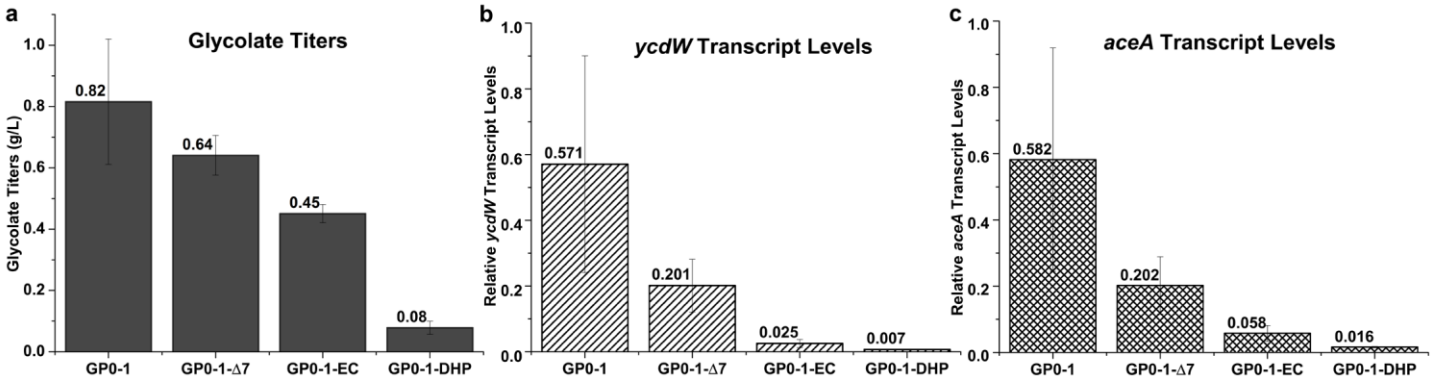
a
Glycolate Titers
Glycolate Titers (g/L)
0.82
0.64
0.45
0.08
GP0-1
GP0-1-Δ7
GP0-1-EC
GP0-1-DHP
b
ycdW Transcript Levels
Relative ycdW Transcript Levels
0.571
0.201
0.025
0.007
GP0-1
GP0-1-Δ7
GP0-1-EC
GP0-1-DHP
c
aceA Transcript Levels
Relative aceA Transcript Levels
0.582
0.202
0.058
0.016
GP0-1
GP0-1-Δ7
GP0-1-EC
GP0-1-DHP

Figure 5

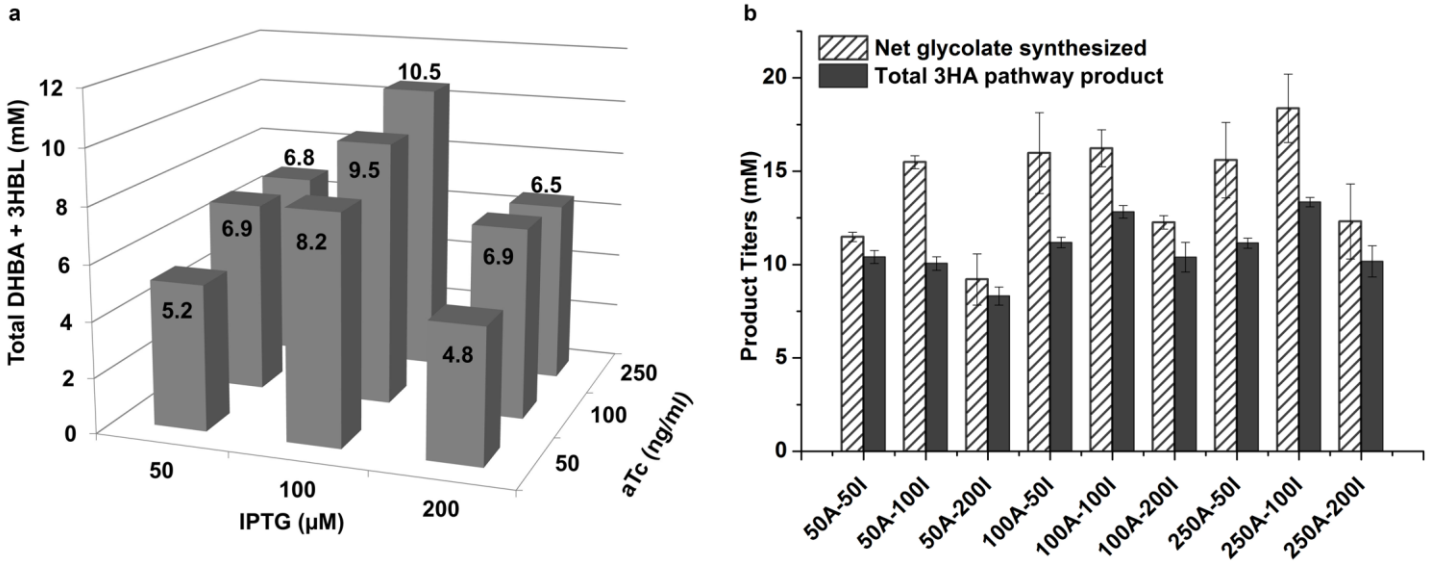
a
Total DHBA + 3HBL (mM)
12
10
8
6
4
2
0
10.5
6.8
9.5
6.5
6.9
8.2
6.9
5.2
4.8
50
100
200
IPTG (μM)
250
100
50
aTc (ng/ml)
b
Net glycolate synthesized
Total 3HA pathway product
Product Titers (mM)
20
15
10
5
0
50A-50I
50A-100I
50A-200I
100A-50I
100A-100I
100A-200I
250A-50I
250A-100I
250A-200I

Figure 6

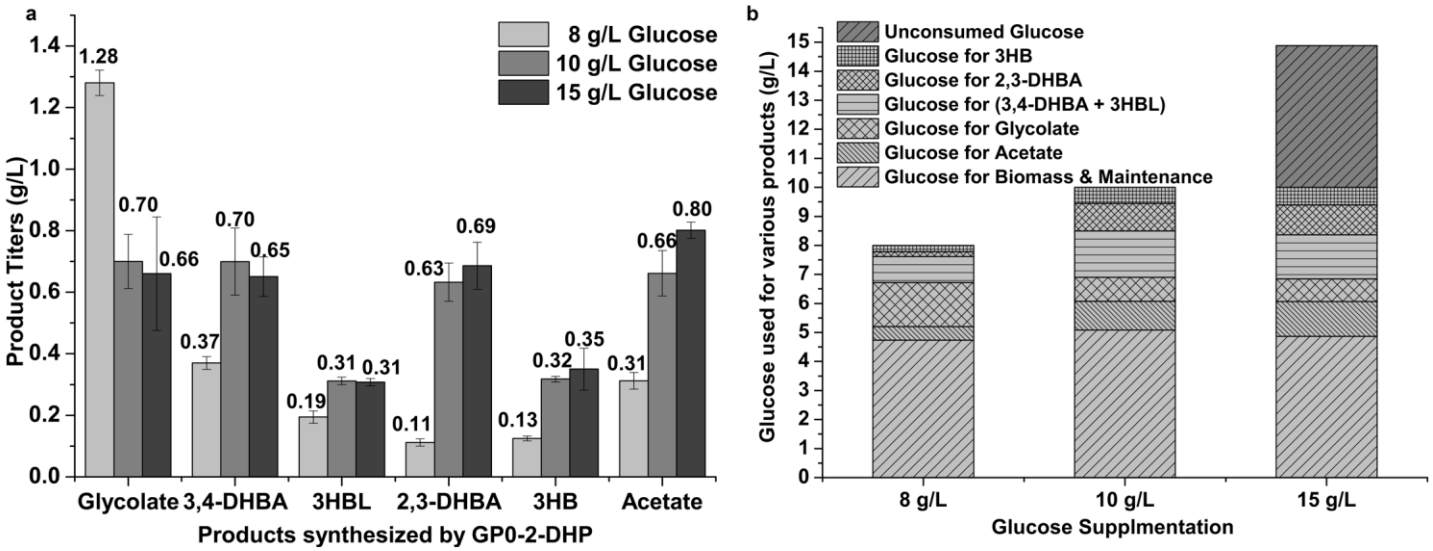
a
8 g/L Glucose
10 g/L Glucose
15 g/L Glucose
Product Titers (g/L)
1.28
0.70
0.66
0.37
0.70
0.65
0.19
0.31
0.31
0.11
0.63
0.69
0.13
0.32
0.35
0.31
0.66
0.80
Glycolate
3,4-DHBA
3HBL
2,3-DHBA
3HB
Acetate
Products synthesized by GP0-2-DHP
b
Unconsumed Glucose
Glucose for 3HB
Glucose for 2,3-DHBA
Glucose for (3,4-DHBA + 3HBL)
Glucose for Glycolate
Glucose for Acetate
Glucose for Biomass & Maintenance
Glucose used for various products (g/L)
8 g/L
10 g/L
15 g/L
Glucose Supplmentation

Table 1 | *E. coli* strains and plasmids

Name	Relevant Genotype	Reference
Strains		
DH10B	F$^-$ *mcr*A Δ(*mrr-hsd*RMS-*mcr*BC) ϕ80*lac*ZΔM15 Δ*lacX74 recA1 endA1 araD139*Δ(*ara, leu*)7697 *galU galK* λ$^-$ *rpsL nupG*	Invitrogen
ElectroTen-Blue	Δ(*mcrA*)*183* Δ*(mcrCB-hsdSMR-mrr)173 endA1 supE44 thi-1 recA1 gyrA96 relA1 lac* Kan^r [F′ *proAB lacI*^{q}ZΔM15 Tn*10* (Tet^r)]	Stratagene
MG1655 (DE3)	F$^-$ λ$^-$ *ilvG- rfb-50 rph-1 with the DE3 prophage integrated*	Tseng 2010
DHP0	MG1655 (DE3) carrying pDHP-1 and pDHP-2	This study
DHP0+*acs*	MG1655 (DE3) carrying pDHP-1 and pDHP-2a	This study
GP0-1	MG1655 (DE3) carrying pGLY-1	This study
GP0-1-DHP	GP0-1 containing pDHP-1 and pDHP-2	This study
GP0-2	MG1655(DE3) carrying pGLY2	This study
GP0-2-DHP	GP0-2 carrying pDHP-1 and pDHP-2	This study
GP0-2-DHP+*acs*	GP0-2 carrying pDHP-1 and pDHP-2a	This study
GP1	MG1655 (DE3) Δ*iclR*	This study
GP2	MG1655 (DE3) Δ*iclR,* Δ*aceB*	This study
GP3	MG1655 (DE3) Δ*iclR,* Δ*aceB,* Δ*gcl*	This study
GP4	MG1655 (DE3) Δ*iclR,* Δ*aceB,* Δ*gcl,* Δ*glcB*	This study
GP1-2	GP1 carrying pGLY-2	This study
GP2-2	GP2 carrying pGLY-2	This study
GP3-2	GP3 carrying pGLY-2	This study
GP4-2	GP4 carrying pGLY-2	This study
GP1-2-DHP	GP1-2 carrying pDHP-1 and pDHP-2	This study
GP2-2-DHP	GP2-2 carrying pDHP-1 and pDHP-2	This study
GP3-2-DHP	GP3-2 carrying pDHP-1 and pDHP-2	This study
GP4-2-DHP	GP4-2 carrying pDHP-1 and pDHP-2	This study
Plasmids		
pETDuet-1	ColE1(pBR322) *ori*, *lacI,* T7*lac*, Amp^R	Novagen
pCDFDuet-1	CloDF13 *ori*, *lacI,* T7*lac*, Strep^R	Novagen
pCOLADuet-1	ColA *ori*, *lacI,* T7*lac*, Kan^R	Novagen
pHHD01K	p15 *ori, tetR,* Ptet, Kan^R	This study
pGLY-1	pCOLADuet-1 harboring *ycdW* and *aceA-aceK* from *E.coli* MG1655	This study
pGLY-2	pHHD01K harboring the genes *ycdW, aceA and aceK* from *E.coli* MG1655 in an artificial operon similar in structure to the *aceBAK* operon	This study
pDHP-1	pETDuet-1 harboring *bktB* and *phaB* from *C.necator* named pET/bktB/phaB in Martin *et al*, 2013	Martin et al, 2013
pDHP-2	pCDFDuet-1 harboring *pct* from *M. elsdenii*, and *tes*B from *E.*	Martin et al,

	coli MG1655 named pCDF/pct/tesB in Martin *et al*, 2013	2013
pDHP-2a	pCDFDuet-1 harboring *pct* from *M. elsdenii*, and an artificial operon of the genes *acs and tes*B from *E. coli* MG1655	This study

SUPPLEMENTARY INFORMATION

For

Engineering *E. coli* for the biosynthesis of 3-hydroxy-γ-butyrolactone (3HBL) and 3,4-dihydroxybutyric acid (3,4-DHBA) as value-added chemicals from glucose as a sole carbon source

Himanshu Dhamankar[a,b], Yekaterina Tarasova[b,c], Collin H. Martin[a,b,1], Kristala L. Jones Prather[a,b,*]

[a] *Department of Chemical Engineering, Massachusetts Institute of Technology, Cambridge, MA 02139* [b] *Synthetic Biology Engineering Research Center (SynBERC), Massachusetts Institute of Technology, Cambridge, MA 02139*

[c] *Microbiology Graduate Program, Massachusetts Institute of Technology, Cambridge, MA 02139*

Submitted for publication in: ***Metabolic Engineering***

[1]Current address:
The Dow Chemical Company, Spring House, PA 19477, USA
* Corresponding author:
Department of Chemical Engineering
77 Massachusetts Avenue, Room E17-504
Cambridge, MA 02139
Phone: 617.253.1950
Fax: 617.258.5042
Email: kljp@mit.edu

Supplementary Figures

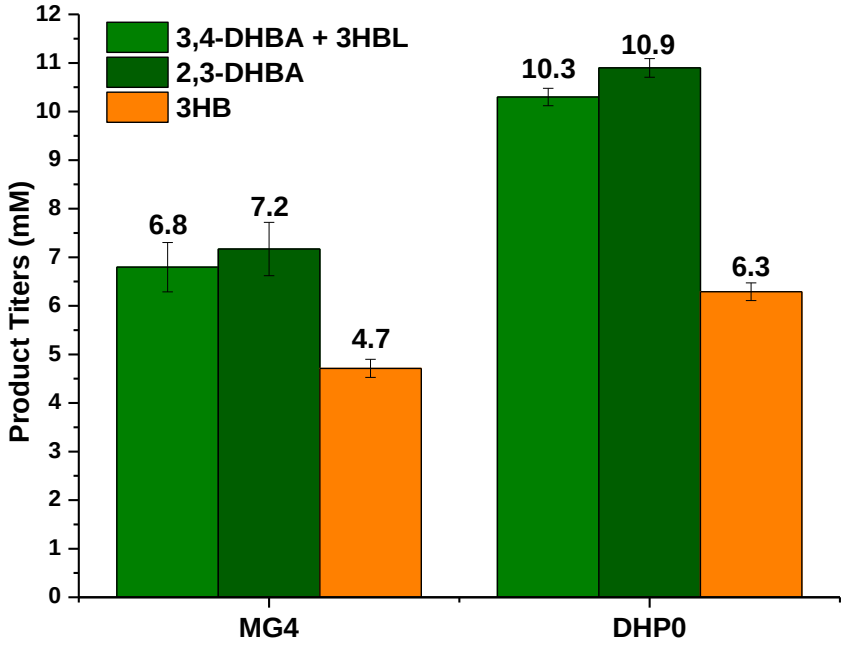

Strain	3,4-DHBA (mg/L)	3HBL (mg/L)	2,3-DHBA (mg/L)	([3,4-DHBA]+[3HBL]) [3HB]	([3,4-DHBA]+[3HBL]) [2,3-DHBA]
MG4 (MG1655 (DE3 *ΔendA ΔrecA*))	555 ± 52	221 ± 15	860 ± 65	2.58	0.95
DHP0 (MG1655 (DE3))	918 ± 12	271 ± 01	1309 ± 23	3.37	0.95

Supplementary Figure S1 | DHBA / 3HBL synthesis by strains MG1655 (DE3 *ΔendA ΔrecA*) and MG1655 (DE3). Strain MG4 has been previously described in Martin et al., 2013, and is essentially strain MG1655 (DE3 *ΔendA ΔrecA*) carrying pDHP-1 and pDHP-2. DHP0 is MG1655 (DE3) carrying pDHP-1 and pDHP-2. Each of the strains was cultured in LB supplemented with 1% glucose and 40 mM glycolate, using the same conditions as reported in Martin et al., 2013. Product titers (in mM) 72 hours post induction are reported.

The *E. coli* K-12 strain MG1655 (DE3) (strain GP0) was selected as the host strain for investigating direct synthesis of DHBA and 3HBL from glucose, owing to its amenability to chromosomal engineering via homologous recombination. We compared DHBA and 3HBL synthesis from exogenously supplied glycolate in this strain transformed with DHBA pathway plasmids (strain DHP0) with that in the previously employed strain MG1655 (DE3 *ΔendA ΔrecA*) carrying the same plasmids (strain MG4, (Martin et al., 2013)) to establish a baseline for the product titers with this strain. It was observed that strain MG1655 (DE3) proved superior to MG1655 (DE3 *ΔendA ΔrecA*) in terms of DHBA and 3HBL synthesis, with 50% higher total DHBA + 3HBL, 34% higher 3HB titers (**Supplementary Figure S1**) and an overall yield of 53% on the supplied glycolate.

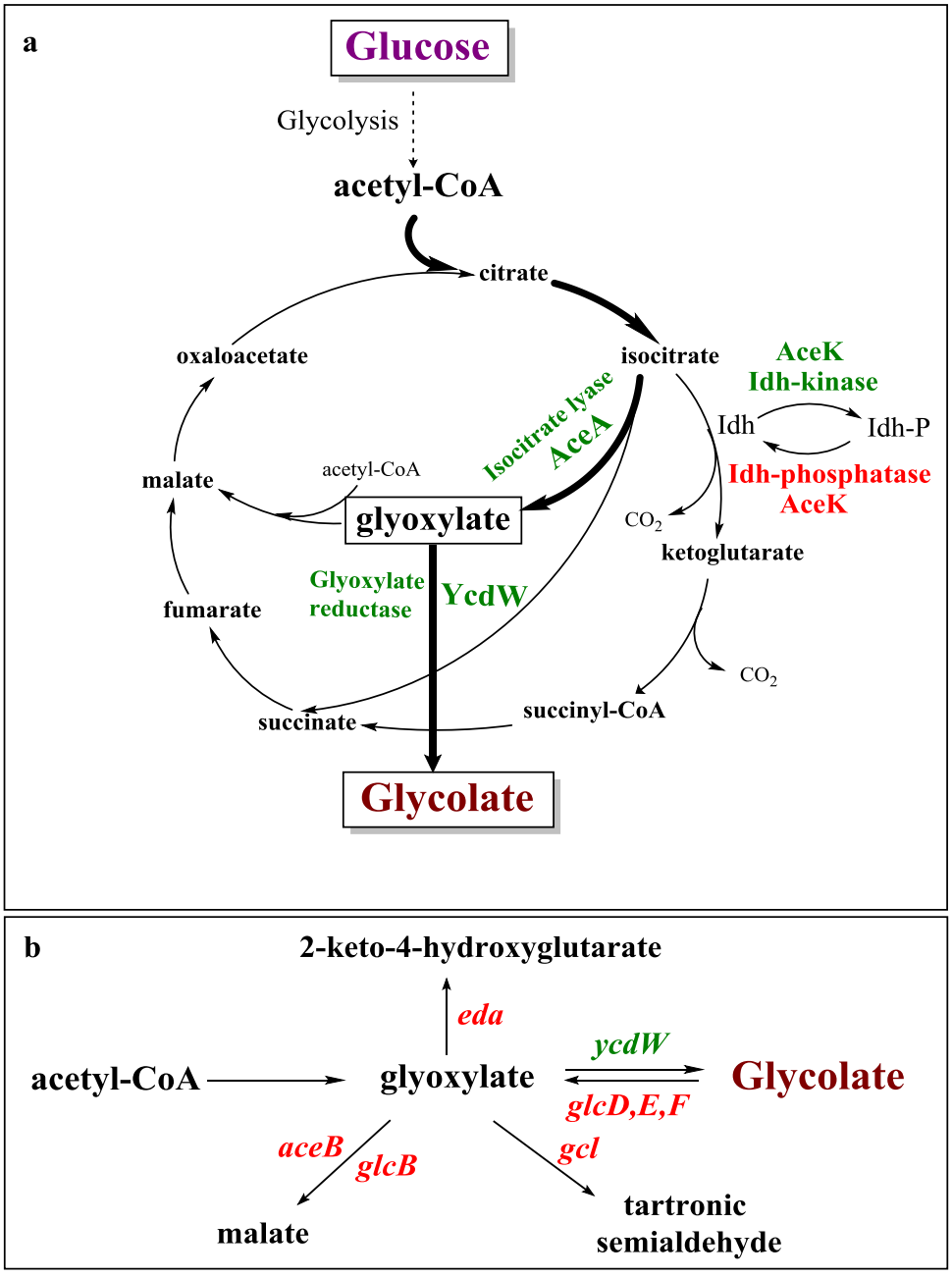

Supplementary Figure S2 | Glycolate synthesis and consumption pathways in *E. coli.* a) Glycolate synthesis via the glyoxylate shunt. During growth on a limited amount of glucose or acetate, Idh-kinase / phosphatase phosphorylates Idh, causing a drop in its activity, thereby reducing isocitrate flux through the TCA cycle. Simultaneous expression of isocitrate lyase (AceA) diverts isocitrate flux through the glyoxylate shunt, synthesizing glyoxylate which is reduced to glycolate by glyoxylate reductase (YcdW). b) Glycolate and glyoxylate are consumed along multiple competing pathways. The enzymes marked in green promote glycolate synthesis while those in red consume glycolate.

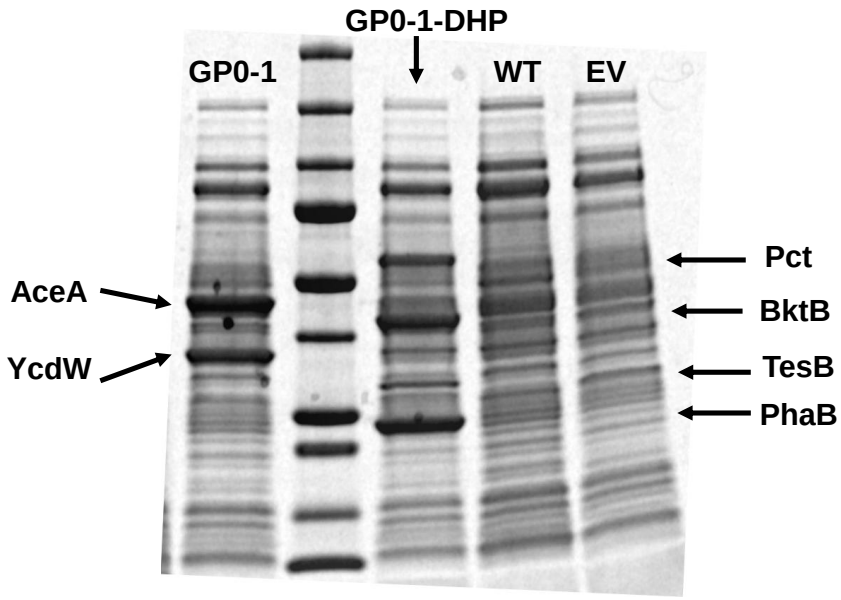

Supplementary Figure S3 | Comparing expression of pathway enzymes in recombinant strains GP0-1, GP0-1-DHP with wild-type and empty vector controls. Protein lysates from wild-type *E. coli* MG1655 and empty plasmid control strain, as well as strains GP0-1 and GP0-DHP, were isolated from cultures grown in M9 minimal medium + 1% glucose. Samples were collected 6 hours post induction with 1 mM IPTG. Cells were lysed with cell disruption beads, clarified, and 15 ug total protein loaded into each lane. EV = MG1655 with empty pETDuet, empty pCDFDuet, and empty pCOLADuet. AceA and YcdW proteins are only overexpressed in the GP0 strain.

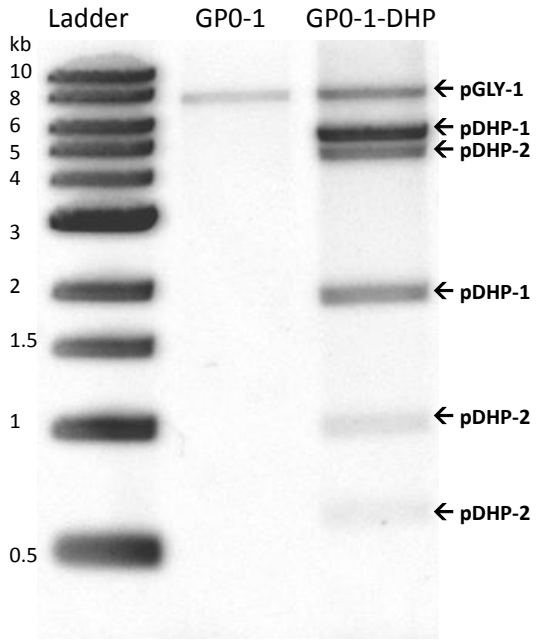

Supplementary Figure S4 | Agarose gel confirming intact plasmids in strains GP0-1 and GP0-1-DHP 1. To rule out the possibility of plasmid loss and/or instability as a cause for decreased glycolate and DHBA synthesis in strain GP0-1-DHP, we performed a standard plasmid extraction on GP0-1-DHP and GP0 strains. We collected ~1 ml of each culture, normalized by OD_{600}, from 50 mL shake flask cultures grown in M9 medium supplemented with 1% glucose, 6 hours post induction with 100 µM IPTG. Plasmid extraction was subsequently performed using a Zymo MiniPrep Kit (Zymo Research, Irvine, CA). Plasmids were eluted with 50 µl of water, of which 5 ul was subjected to digestion with NcoI for 2 hours at 37°C. Digests were run on a 1% agarose gel. The gel was stained with ethidium bromide and imaged using low exposure to avoid saturation. Densitometry analysis was performed using ImageJ (http://imagej.nih.gov/ij/docs/guide). The background was subtracted at a level of 100 pixels. Resulting peaks were integrated and peak areas corresponding to a given plasmid summed and divided by total plasmid size. Each summed peak area was normalized to the brightest band/largest area to obtain relative ratios of plasmids. No plasmid loss of pGLY-1 is evident in GP0-1-DHP relative to DP0-1, and the approximate distribution of plasmids in strain GP0-1-DHP is, pDHP-1 : pDHP-2 : pGLY-1 = 1 : 0.62 : 0.26

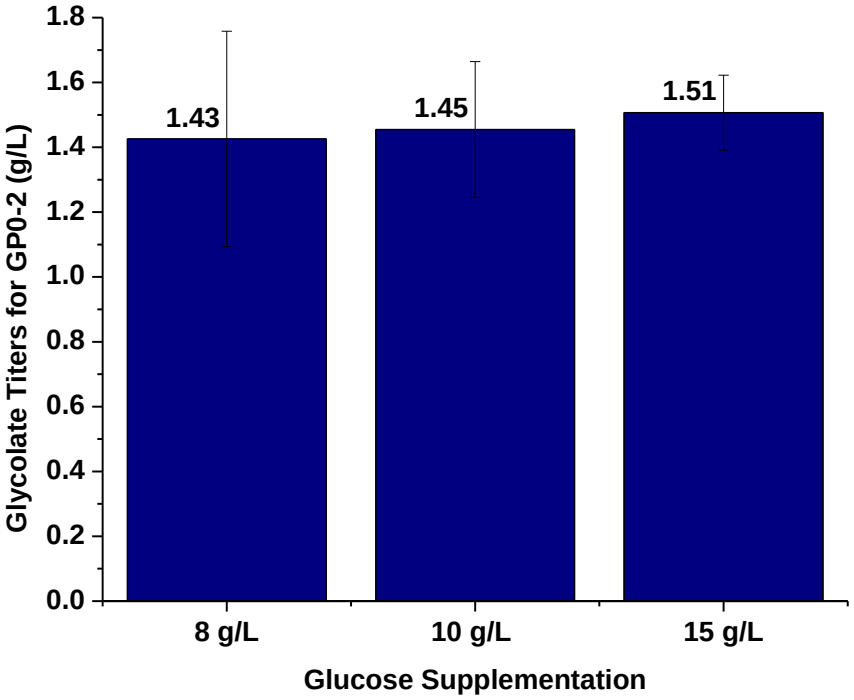

Supplementary Figure S5 | Glycolate synthesis by strain GP0-2. Glycolate titers 72 hours post induction for GP0-2 cultured in M9 minimal medium supplemented with different amounts of glucose and induced with 250 ng/ml aTc.

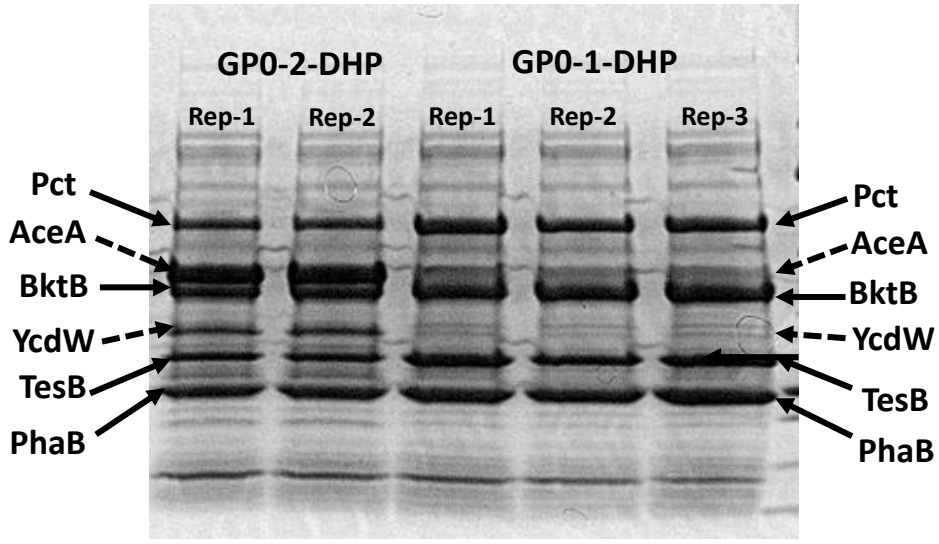

Supplementary Figure S6 | Comparing expression of pathway enzymes in recombinant strains GP0-2-DHP and GP0-1-DHP. Protein lysates from strains GP0-2-DHP and GP0-1-DHP, grown in minimal medium supplemented with 1% glucose and induced with 250 ng/ml aTc and 100 µM IPTG (for GP0-2-DHP) or only 100 µM IPTG (for GP0-1-DHP) were loaded on a SDS-PAGE gel for separation. From the left, lanes 1-2 show lysates from GP0-2-DHP cultures (2 replicates) while lanes 3-5 show lysates from GP0-1-DHP. While GP0-2-DHP shows over-expression of the glycolate pathway enzymes YcdW and AceA in addition to the DHBA/3HBL pathway enzymes Pct, BktB, PhaB and TesB, GP0-1-DHP only shows over-expression of the DHBA/3HBL pathway enzymes, with only faint bands corresponding to AceA and YcdW.

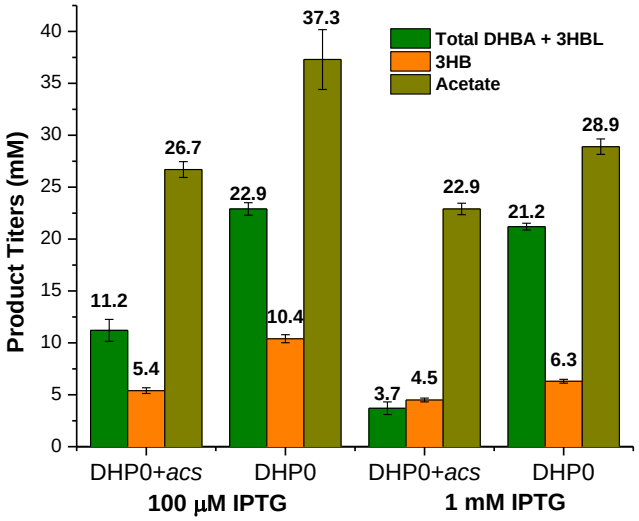

Supplementary Figure S7 | DHBA and 3HBL synthesis with and without Acs expression. Product titers, 72 hours post induction are reported for comparison at two different IPTG induction levels (100 μM and 1 mM) for strains DHP0+*acs* and DHP0.

Strains:
DHP0+*acs* = MG1655(DE3) carrying pDHP-1 and pDHP-2a, expressing Pct, BktB, PhaB, TesB and Acs.
DHP0 = MG1655(DE3) carrying pDHP-1 and pDHP-2a, expressing Pct, BktB, PhaB and TesB.

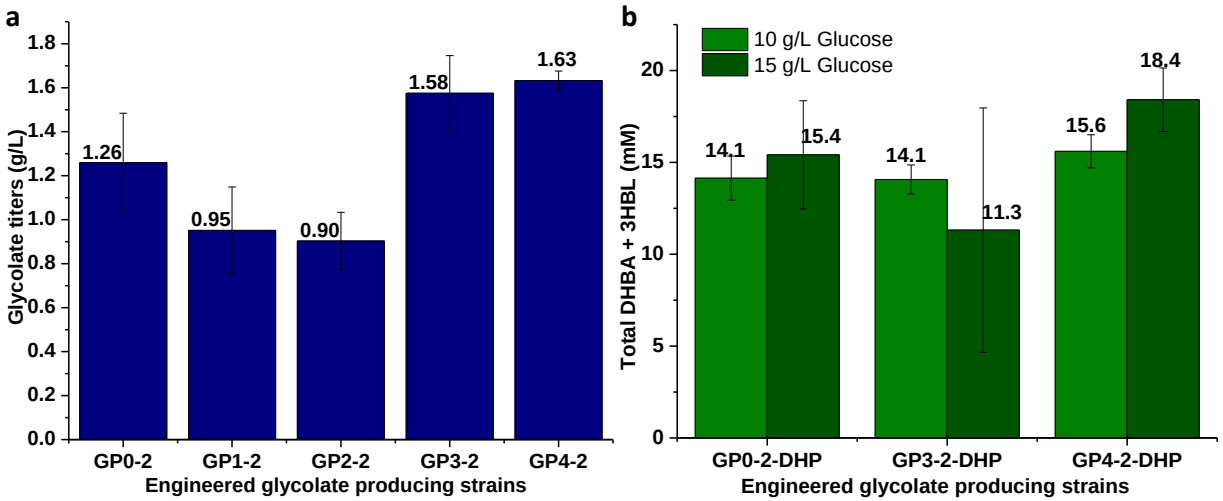

Supplementary Figure S8 | Comparing Glycolate, DHBA and 3HBL synthesis in engineered strains. a) Glycolate titers, 72 hours post induction for engineered strains cultured in M9 minimal medium supplemented with 10 g/L glucose, induced with 250 ng/mL aTc. **b)** Total DHBA + 3HBL titers (mM), 72 hours post induction for engineered strains cultured in M9 minimal medium supplemented with 10 g/L glucose, induced with 250 ng/mL aTc and 100 µM IPTG.

Strains:
GP0 = MG1655 (DE3)
GP1 = MG1655 (DE3 *ΔiclR*)
GP2 = MG1655 (DE3 *ΔiclR Δgcl*)
GP3 = MG1655 (DE3 *ΔiclR Δgcl ΔaceB*)
GP4 = MG1655 (DE3 *ΔiclR ΔaceB Δgcl ΔglcB*)

GP0-2 to GP4-2= Strains GP0 to GP4 carrying pGLY-2
GP0-2-DHP to GP4-2-DHP= Strains GP0 to GP4 carrying pDHP-1, pDHP-2 and pGLY-2.

We investigated glycolate, DHBA and 3HBL synthesis with *ycdW*, *aceA* and *aceK* over-expression in strains engineered to eliminate different endogenous glycolate and glyoxylate consumption pathways (strains GP1, GP2, GP3 and GP4). This approach had previously resulted in improved glycolate synthesis when used in combination with over-expression of *ycdW* alone (Soucaille, 2009). The *iclR* knockout by itself was observed to be detrimental to glycolate synthesis (strain GP1-2), indicating that the expected improvement in endogenous *aceA* and *aceK* expression with this knockout was insignificant in comparison to the over-expression from pGLY-2. Only strains GP3 and GP4 showed improved glycolate synthesis in M9-glucose cultures in comparison to the parent strain GP0, with 20-30% higher glycolate titers at the shake flask scale (**Supplementary Figure S8a**). However, these strains did not show appreciably improved DHBA and 3HBL synthesis (**Supplementary Figure S8b**). While we have not evaluated all possible knockout combinations exhaustively, these results suggest that over-expression of *ycdW*, *aceA* and *aceK* alone allows sufficient glycolate synthesis in the base strain GP0, with

glycolate and glyoxylate consumption not being significantly limiting at the shake flask scale. These preliminary observations warrant a more detailed study of these and other engineered strains at the bioreactor scale.

Supplementary Methods

Supplementary Table S1 | List of DNA oligonucleotide primers used in the cloning of genes and for qPCR reactions

Primer names correspond to the name of the gene or vector backbone that the primer amplifies, whether the primer is the forward primer (FP) or reverse primer (RP) of that gene or vector, and the restriction site incorporated into the primer sequence (in case of a primer used to generate a fragment for cloning). For primers used to amplify the *acs* and *tesB* genes from *E. coli* for the construction of the *acs-tesB* operon, sequences indicated in bold correspond to parts of the complementary overlapping regions for SOEing PCR.

Primer	Sequence 5'→3'	Source
ycdW-FP-NdeI	TAAAAACATATGGATATCATCTTTTATCACCCAACG	Sigma-Genosys
ycdW-RP-XhoI	TAAAAACTCGAGTTAGTAGCCGCGTGCG	Sigma-Genosys
aceAK-FP-NcoI	TAAAAACCATGGGCATGGAGCATCTGCAC	Sigma-Genosys
aceAK-RP-EcoRI	TAAAAAGAATTCTCAAAAAAGCATCTCCCCATAC	Sigma-Genosys
pETDuet-ΔT7-FP-XmaI	GAAAAAACCCGGGGGCAGATCTCAATTGGATATCGG	Sigma-Genosys
pETDuet-ΔT7-RP-XmaI	GAAAAAACCCGGGGATCTCGATCCTCTACGCCG	Sigma-Genosys
pCDFDuet-ΔT7-FP-XmaI	GAAAAAACCCGGGGGCAGATCTCAATTGGATATCGG	Sigma-Genosys
pCDFDuet-ΔT7-RP-XmaI	GAAAAAACCCGGGGAGTCGCATAAGGGAGAGCGTC	Sigma-Genosys
ycdW-qPCR-FP	CACATGTCGCCGCGATT	Sigma-Genosys
ycdW-qPCR-RP	GGCAATGGTGCGAGAAATGTA	Sigma-Genosys
aceA-qPCR-FP	ACCGGCGAGCGTACCA	Sigma-Genosys
aceA-qPCR-RP	CCAGGCCACGGCTGATC	Sigma-Genosys
NdeI-*acs*-FP	TAAAAACATATGAGCCAAATTCACAAACACAC	Sigma-Genosys
acs-RP	**TATATATCTCCTTCTTATTTACGATGGCATC**GCGATAG	Sigma-Genosys
tesB-FP	**GATGCCATCGTAAATAAGAAGGAGATATATA**ATGAGTCAGG CGATAAAAAATTTAC	Sigma-Genosys
PacI-*tesB*-RP	TAAAAAAATTAATTGTGATTACGCATCACCC	Sigma-Genosys

Supplementary Table S2 | Molar yields and selectivity in the synthesis of 3,4-DHBA and 3HBL from glucose

Supplied Glucose	Molar Yield (3,4-DHBA + 3HBL) on Glucose*	% of Theoretical Pathway Yield	$\frac{([DHBA]+[3HBL])}{[3HB]}$	$\frac{([3,4\text{-}DHBA]+[3HBL])}{([2,3\text{-}DHBA]+[3HB])}$	$\frac{([3,4\text{-}DHBA]+[3HBL])}{[2,3\text{-}DHBA]}$
8 g/L	0.112	17.0	4.93 ± 0.32	2.35 ± 0.23	5.41 ± 0.68
10 g/L	0.160	24.2	4.63 ± 0.26	1.07 ± 0.09	1.69 ± 0.18
15 g/L	0.152	23.0	4.26 ± 0.41	0.93 ± 0.07	1.48 ± 0.09

* Molar yield is calculated as ratio of moles of 3,4-DHBA + 3HBL synthesized to moles of glucose consumed and does not include 2,3-DHBA. The total molar pathway yield values including 2,3-DHBA are 0.148, 0.285 and 0.274 respectively for 8, 10 and 15 g/L of supplied glucose and amount to 22.4%, 43.2% and 41.5% of the theoretical maximum yield.

Supplementary Table S3 | Product Titers (mM) for different concentrations of supplied glucose

Supplied Glucose	3,4-DHBA (mM)	3HBL (mM)	2,3-DHBA (mM)	3HB (mM)	Glycolate (mM)	Acetate (mM)	Unconsumed Glucose (mM)
8 g/L	3.1 ± 0.2	1.9 ± 0.2	0.9 ± 0.1	2.35 ± 0.5	2.0 ± 0.1	5.2 ± 0.5	0.0 ± 0.0
10 g/L	5.8 ± 0.9	3.1 ± 0.1	5.3 ± 0.5	1.07 ± 1.0	3.1 ± 0.1	11.0 ± 1.2	0.0 ± 0.0
15 g/L	5.4 ± 0.5	3.0 ± 0.1	5.7 ± 0.6	0.93 ± 2.4	3.4 ± 0.7	13.4 ± 0.4	27.1 ± 3.5

Supplementary Table S4 | Molar distribution of supplied glucose in the synthesis of different products*

Supplied Glucose	Glucose for 3,4-DHBA + 3HBL (mM)	Glucose for 2,3-DHBA (mM)	Glucose for 3HB (mM)	Glucose for Glycolate (mM)	Glucose for Acetate (mM)	Unconsumed Glucose (mM)	Glucose for B&M** (mM)
8 g/L (44.4 mM)	5.0	0.9	1.2	8.4	2.6	0	26.3
10 g/L (55.5 mM)	8.9	5.3	3.1	4.6	5.5	0	28.2
15 g/L (83.3 mM)	8.4	5.7	3.4	4.3	6.7	27.1	27.7

* The glucose consumed theoretically in the formation of each of the products in the above table is estimated using the product titers from **Supplementary Table S3** and the stoichiometric coefficients from the above listed theoretical reactions.

** Glucose for B&M = Glucose for Biomass and Maintenance functions and is calculated as the difference between the supplied glucose and the sum of the glucose consumed theoretically for the formation of different products and the unconsumed glucose.

Supplementary Calculations

Net Reactions and Theoretical Yield Calculations - Synthesis of DHBA, 3HBL and other products from glucose

Calculation of pathway independent theoretical maximum yield on glucose (Y^E)

The pathway independent maximum yield (Y^E), is a measure of the most efficient conversion of a given substrate into a product along a hypothetical (or real) route that is redox neutral and hence captures all the energy of the starting substrate into the product (Dugar and Stephanopoulos, 2011). For DHBA synthesis from glucose, the net reaction for this conversion is:

Thus, Y^E **= Degree of reductance for glucose / degree of reductance of 3,4-DHBA**
= (6x4 + 12x1 – 6x2) / (4x4 + 8x1-4x2)
= 24/16 = 1.5 moles DHBA / mole of glucose

Calculation of maximum theoretical pathway yield (Y^P)

Pathway Reactions (without acetate recycling)

Glycolate synthesis:

½ Glucose + ADP + P_i + $3NAD^+$ + FAD + NADPH + CoASH ⟶ Glycolate + CO_2 + ATP + $FADH_2$ + 3NADH +NADP + CoASH

DHBA / 3HBL synthesis:

Glucose + Glycolate + 2ADP + $2P_i$ + $4NAD^+$ + NADPH + 2CoASH ⟶ 3,4-DHBA + $2CO_2$ + Acetate + 2ATP + 4NADH + NAPD + 2CoASH

Net Reaction:

3/2 Glucose + 3ADP + $3P_i$ + $7NAD^+$ + 2NADPH +FAD+ 3CoASH ⟶ 3,4-DHBA + $3CO_2$ + Acetate + 3ATP + + 7NADH +2NAPD +$FADH_2$ + 3CoASH

Theoretical pathway yield $Y^P_{w/o\text{-}acetate\text{-}recycling}$ **= 0.67 moles 3,4-DHBA / mole of glucose**

The net reaction above shows that the pathway results in the synthesis of an excess of reducing equivalents which affect the overall yield. Separate reactions for regeneration of NADPH are not taken into account, assuming that the excess of NADH synthesized can supply some of the NADPH requirement through inter-conversion by transhydrogensases.

For every mole of 3,4-DHBA synthesized, a mole of acetate is formed as a by-product. The pathway above also shows an excess of reducing equivalents and ATP synthesis. Recycling acetate into acetyl-CoA by activation with acetyl-CoA synthetase (Acs) using this excess of ATP can help improve the maximum theoretical pathway yield as below.

Pathway Reactions (with acetate recycling)

Net Reaction:

Glucose + ADP + P_i + 5NAD^+ + 2NADPH + FAD+ 2CoASH ⟶ 3,4-DHBA + 2CO_2 + ATP + 5NADH +2NAPD + $FADH_2$ + 2CoASH

Theoretical pathway yield $Y^P_{with\text{-}acetate\text{-}recycling}$ **= 1.0 moles 3,4-DHBA / mole of glucose**

3HB synthesis reaction:

Net Reaction:

Glucose + 2ADP + 2P_i + 4NAD^+ + NADPH + 4CoASH ⟶ 3HB + 2CO_2 + 2ATP + 4NADH +NAPD + 4CoASH

2,3-DHBA synthesis reaction:

Net Reaction:

3/2Glucose + ADP + P_i + 5NAD^+ + 2NADPH + FAD+ 2CoASH ⟶ 2,3-DHBA + 2CO_2 + ATP + 5NADH +2NAPD + $FADH_2$ + 2CoASH

Supplementary References

Dugar, D., Stephanopoulos, G., 2011. Relative potential of biosynthetic pathways for biofuels and bio-based products. Nature Biotechnology. 29**,** 1074-1078.

Martin, C. H., Dhamankar, H., Tseng, H.-C., Sheppard, M. J., Reisch, C. R., Prather, K. L. J., 2013. A platform pathway for production of 3-hydroxyacids provides a biosynthetic route to 3-hydroxy-gamma-butyrolactone. Nature Communications. 4**,** 1-7.

Soucaille, P., Glycolic acid production by fermentation from renewable resources. In: Office, U. S. P., (Ed.), United States, 2009.

SUPPLEMENTARY INFORMATION

For

Engineering *E. coli* for the biosynthesis of 3-hydroxy-γ-butyrolactone (3HBL) and 3,4-dihydroxybutyric acid as ~~a~~ value-added chemicals from glucose as a sole carbon source

Himanshu Dhamankar[a,b], Yekaterina Tarasova[b,c], Collin H. Martin[a,b,1], Kristala L. Jones Prather[a,b,*]

[a] *Department of Chemical Engineering, Massachusetts Institute of Technology, Cambridge, MA 02139* [b] *Synthetic Biology Engineering Research Center (SynBERC), Massachusetts Institute of Technology, Cambridge, MA 02139*

[c] *Microbiology Graduate Program, Massachusetts Institute of Technology, Cambridge, MA 02139*

Submitted for publication in: ***Metabolic Engineering***

[1]Current address:
The Dow Chemical Company, Spring House, PA 19477, USA
* Corresponding author:
Department of Chemical Engineering
77 Massachusetts Avenue, Room E17-504
Cambridge, MA 02139
Phone: 617.253.1950
Fax: 617.258.5042
Email: kljp@mit.edu

Supplementary Figures

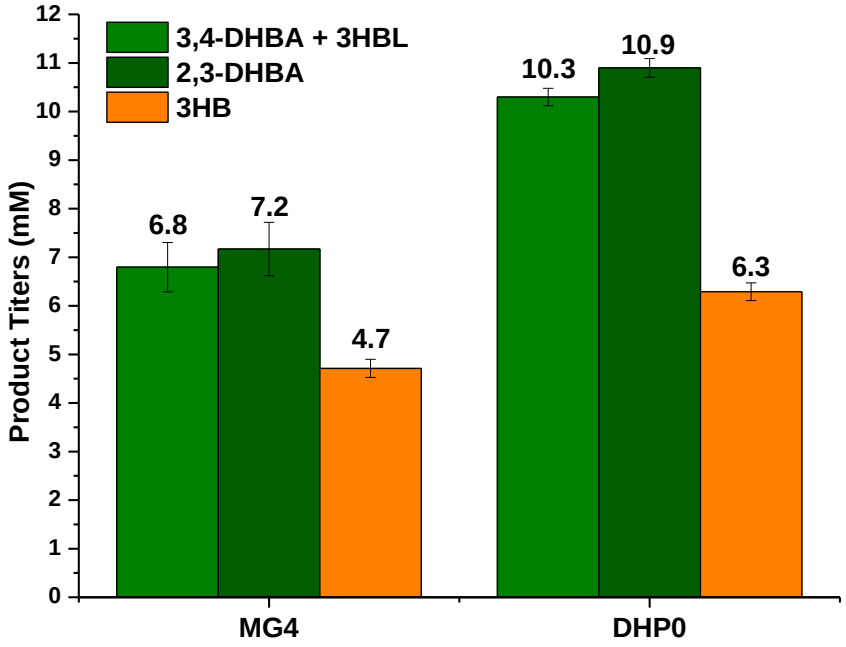

Strain	3,4-DHBA (mg/L)	3HBL (mg/L)	2,3-DHBA (mg/L)	([3,4-DHBA]+[3HBL]) [3HB]	([3,4-DHBA]+[3HBL]) [2,3-DHBA]
MG4 (MG1655 (DE3 *ΔendA ΔrecA*))	555 ± 52	221 ± 15	860 ± 65	2.58	0.95
DHP0 (MG1655 (DE3))	918 ± 12	271 ± 01	1309 ± 23	3.37	0.95

Supplementary Figure S1 | DHBA / 3HBL synthesis by strains MG1655 (DE3 *ΔendA ΔrecA*) and MG1655 (DE3). Strain MG4 has been previously described in Martin et al., 2013, and is essentially strain MG1655 (DE3 *ΔendA ΔrecA*) carrying pDHP-1 and pDHP-2. DHP0 is MG1655 (DE3) carrying pDHP-1 and pDHP-2. Each of the strains was cultured in LB supplemented with 1% glucose and 40 mM glycolate, using the same conditions as reported in Martin et al., 2013. Product titers (in mM) 72 hours post induction are reported.

The *E. coli* K-12 strain MG1655 (DE3) (strain GP0) was selected as the host strain for investigating direct synthesis of DHBA and 3HBL from glucose, owing to its amenability to chromosomal engineering via homologous recombination. We compared DHBA and 3HBL synthesis from exogenously supplied glycolate in this strain transformed with DHBA pathway plasmids (strain DHP0) with that in the previously employed strain MG1655 (DE3 *ΔendA ΔrecA*) carrying the same plasmids (strain MG4, (Martin et al., 2013)) to establish a baseline for the product titers with this strain. It was observed that strain MG1655 (DE3) proved superior to MG1655 (DE3 *ΔendA ΔrecA*) in terms of DHBA and 3HBL synthesis, with 50% higher total DHBA + 3HBL, 34% higher 3HB titers (**Supplementary Figure S1**) and an overall yield of 53% on the supplied glycolate.

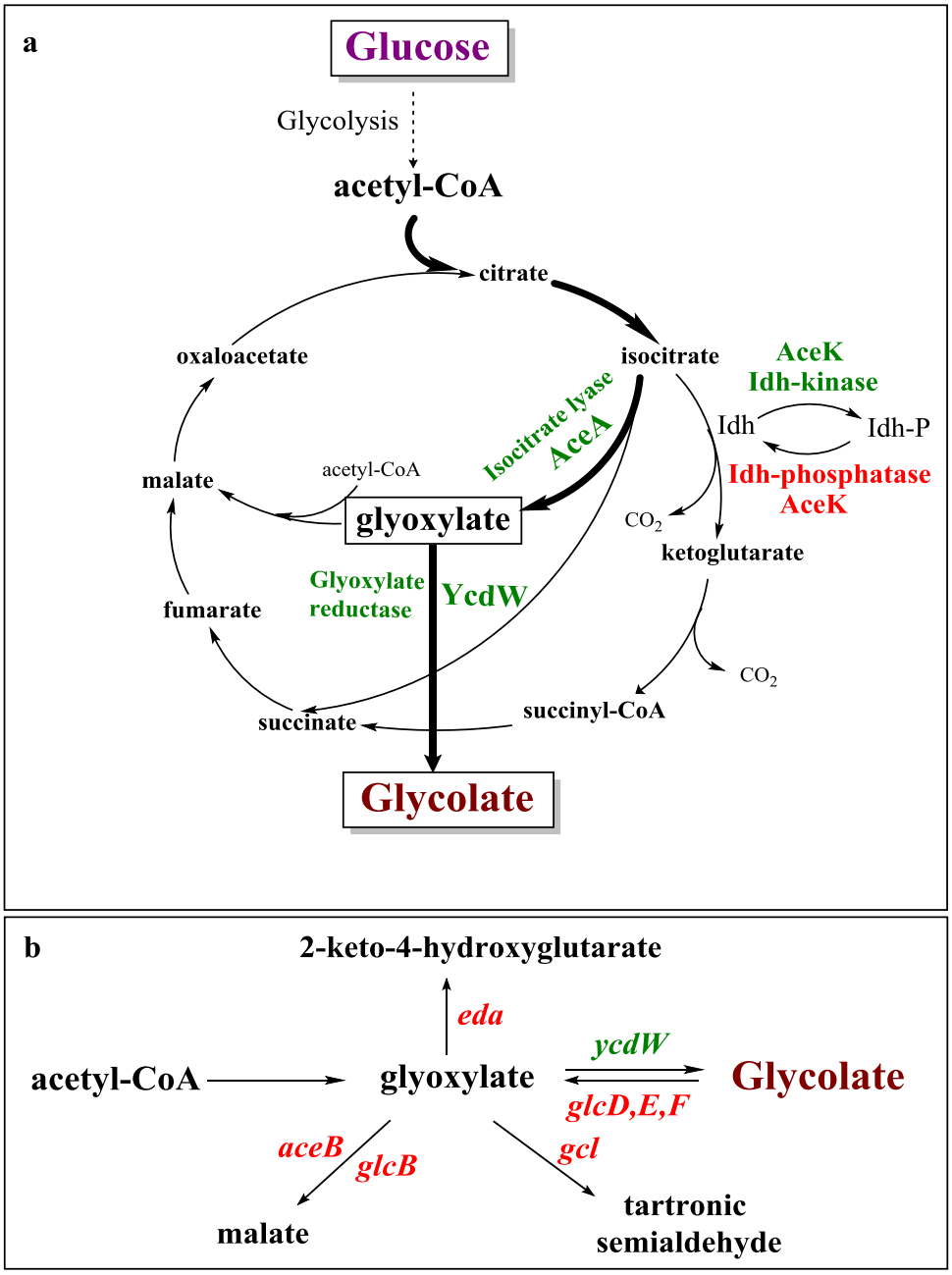

Supplementary Figure S2 | Glycolate synthesis and consumption pathways in *E. coli.* a) Glycolate synthesis via the glyoxylate shunt. During growth on limited amount of glucose or acetate, Idh-kinase / phosphatase phosphorylates Idh, causing a drop in its activity, thereby reducing isocitrate flux through the TCA cycle. Simultaneous expression of isocitrate lyase (AceA) diverts isocitrate flux through the glyoxylate shunt, synthesizing glyoxylate which is reduced to glycolate by glyoxylate reductase (YcdW). b) Glycolate and glyoxylate are consumed along multiple competing pathways. The enzymes marked in green promote glycolate synthesis while those in red consume glycolate.

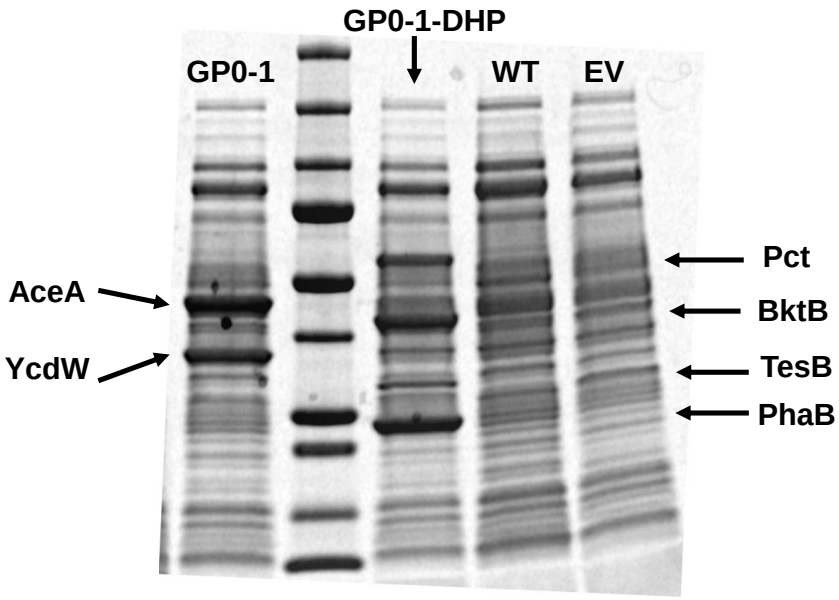

Supplementary Figure S3 | Comparing expression of pathway enzymes in recombinant strains GP0-1, GP0-1-DHP with wild-type and empty vector controls. Protein lysates from wild-type *E. coli* MG1655 and empty plasmid control strain, as well as strains GP0-1 and GP0-DHP, were isolated from cultures grown in M9 minimal medium + 1% glucose. Samples were collected 6 hours post induction with 1 mM IPTG. Cells were lysed with cell disruption beads, clarified, and 15 ug total protein loaded into each lane. EV = MG1655 with empty pETDuet, empty pCDFDuet, and empty pCOLADuet. AceA and YcdW proteins are only overexpressed in the GP0 strain.

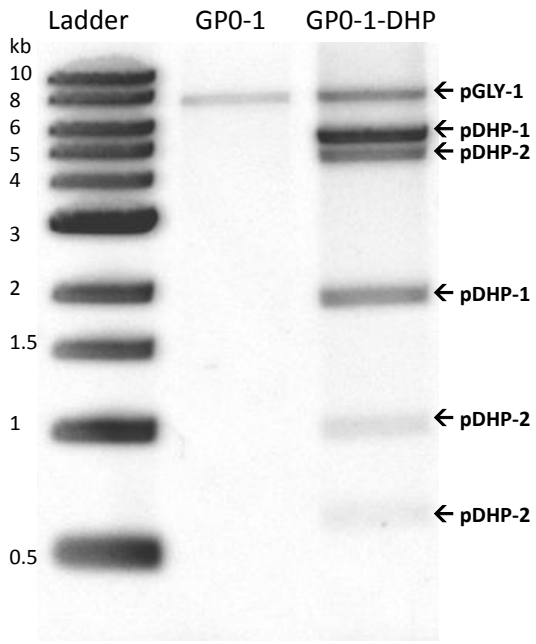

Supplementary Figure S4 | Agarose gel confirming intact plasmids in strains GP0-1 and GP0-1-DHP 1. To rule out the possibility of plasmid loss and/or instability as a cause for decreased glycolate and DHBA synthesis in strain GP0-1-DHP, we performed a standard plasmid extraction on GP0-1-DHP and GP0 strains. We collected ~1 ml of each culture, normalized by OD_{600}, from 50 mL shake flask cultures grown in M9 medium supplemented with 1% glucose, 6 hours post induction with 100 µM IPTG. Plasmid extraction was subsequently performed using a Zymo MiniPrep Kit (Zymo Research, Irvine, CA). Plasmids were eluted with 50 µl of water, of which 5 ul was subjected to digestion with NcoI for 2 hours at 37°C. Digests were run on a 1% agarose gel. The gel was stained with ethidium bromide and imaged using low exposure to avoid saturation. Densitometry analysis was performed using ImageJ (http://imagej.nih.gov/ij/docs/guide). The background was subtracted at a level of 100 pixels. Resulting peaks were integrated and peak areas corresponding to a given plasmid summed and divided by total plasmid size. Each summed peak area was normalized to the brightest band/largest area to obtain relative ratios of plasmids. No plasmid loss of pGLY-1 is evident in GP0-1-DHP relative to DP0-1, and the approximate distribution of plasmids in strain GP0-1-DHP is, pDHP-1 : pDHP-2 : pGLY-1 = 1 : 0.62 : 0.26

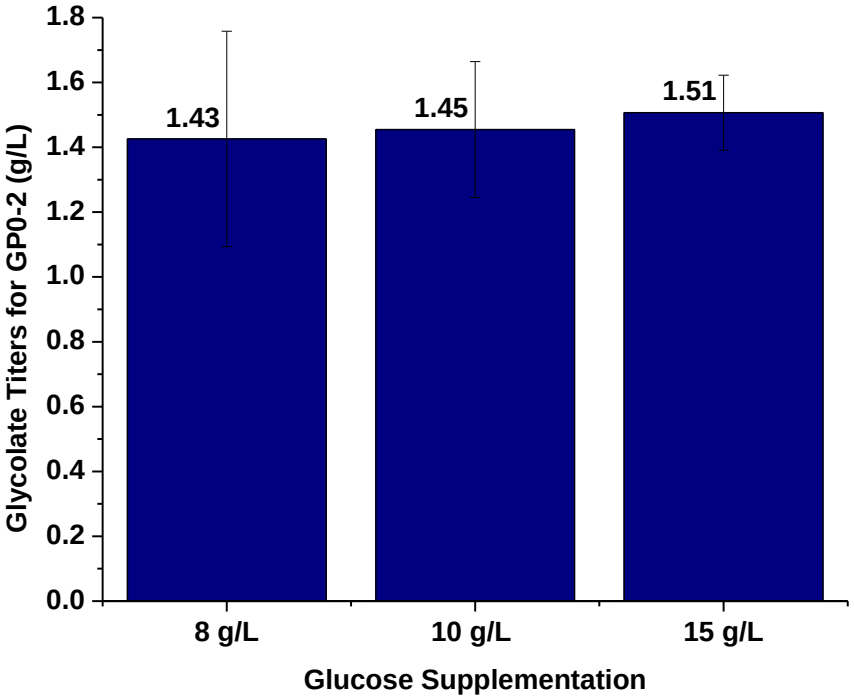

Supplementary Figure S~~3~~5 | Glycolate synthesis by strain GP0-2. Glycolate titers 72 hours post induction for GP0-2 cultured in M9 minimal medium supplemented with different amounts of glucose and induced with 250 ng/ml aTc.

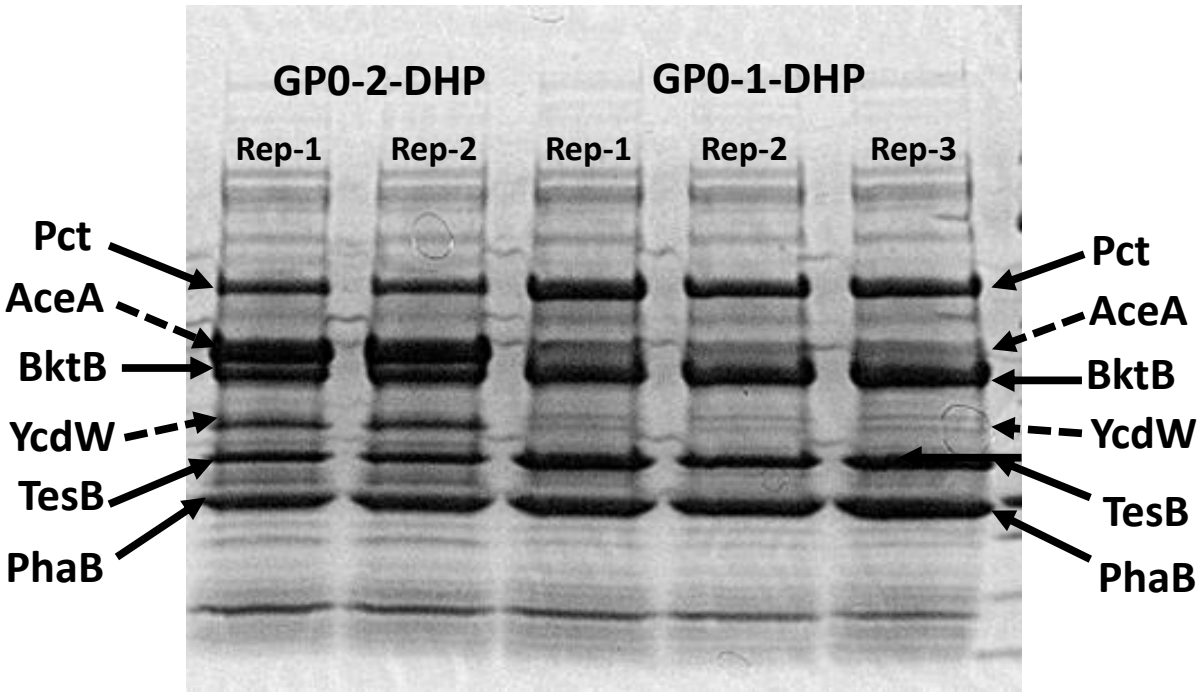

Supplementary Figure S46 | Comparing expression of pathway enzymes in recombinant strains GP0-2-DHP and GP0-1-DHP. Protein lysates isolated from strains GP0-2-DHP and GP0-1-DHP, grown in minimal medium supplemented with 1% glucose and induced with 250 ng/ml aTc and 100 µM IPTG (for GP0-2-DHP) or only 100 µM IPTG (for GP0-1-DHP) were loaded on a SDS-PAGE gel for separation. From the left, lanes 1-2 show lysates from GP0-2-DHP cultures (2 replicates) while lanes 3-5 show lysates from GP0-1-DHP. While GP0-2-DHP shows over-expression of the glycolate pathway enzymes YcdW and AceA in addition to the DHBA/3HBL pathway enzymes Pct, BktB, PhaB and TesB, GP0-1-DHP only shows over-expression of the DHBA/3HBL pathway enzymes, with only faint bands corresponding to AceA and YcdW.

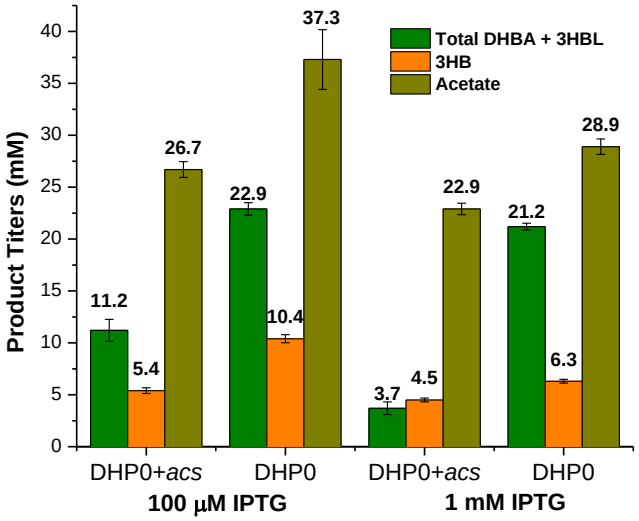

Supplementary Figure ~~S5~~S7 | DHBA and 3HBL synthesis with and without Acs expression. Product titers, 72 hours post induction are reported for comparison at two different IPTG induction levels (100 µM and 1 mM) for strains DHP0+*acs* and DHP0.

Strains:
DHP0+*acs* = MG1655(DE3) carrying pDHP-1 and pDHP-2a, expressing Pct, BktB, PhaB, TesB and Acs.
DHP0 = MG1655(DE3) carrying pDHP-1 and pDHP-2a, expressing Pct, BktB, PhaB and TesB.

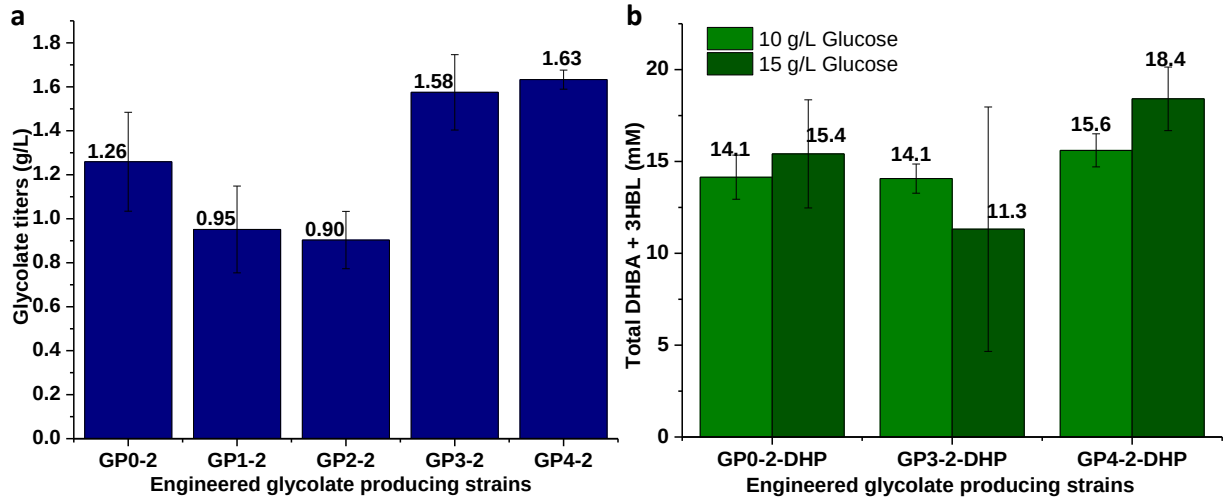

Supplementary Figure S~~8~~6 | Comparing Glycolate, DHBA and 3HBL synthesis in engineered strains. **a)** Glycolate titers, 72 hours post induction for engineered strains cultured in M9 minimal medium supplemented with 10 g/L glucose, induced with 250 ng/mL aTc. **b)** Total DHBA + 3HBL titers (mM), 72 hours post induction for engineered strains cultured in M9 minimal medium supplemented with 10 g/L glucose, induced with 250 ng/mL aTc and 100 µM IPTG. Of the different strains tested, strains GP3 and GP4 showed improved glycolate synthesis in M9-glucose cultures in comparison to the parent strain GP0 (20-30% higher glycolate titers) at the shake flask scale. These strains were then compared with GP0 for DHBA and 3HBL synthesis. While strain GP4-2-DHP showed improved DHBA and 3HBL synthesis as compared to GP0, in M9 cultures supplemented with 15 g/L of glucose, with the average total DHBA + 3HBL titers roughly 20% higher, these differences may not be statistically significant. These preliminary observations warrant a more detailed study of strain GP4, in particular at the bioreactor scale.

Strains:
GP0 = MG1655 (DE3)
GP1 = MG1655 (DE3 *ΔiclR*)
GP2 = MG1655 (DE3 *ΔiclR Δgcl*)
GP3 = MG1655 (DE3 *ΔiclR Δgcl ΔaceB*)
GP4 = MG1655 (DE3 *ΔiclR ΔaceB Δgcl ΔglcB*)

GP0-2 to GP4-2= Strains GP0 to GP4 carrying pGLY-2
GP0-2-DHP to GP4-2-DHP= Strains GP0 to GP4 carrying pDHP-1, pDHP-2 and pGLY-2.

We investigated glycolate, DHBA and 3HBL synthesis with *ycdW*, *aceA* and *aceK* over-expression in strains engineered to eliminate different endogenous glycolate and glyoxylate consumption pathways (strains GP1, GP2, GP3 and GP4). This approach had previously resulted in improved glycolate synthesis when used in combination with over-expression of *ycdW* alone (Soucaille, 2009). The *iclR* knockout by itself was observed to be detrimental to glycolate synthesis (strain GP1-2), indicating that the expected improvement in endogenous *aceA* and

aceK expression with this knockout was insignificant in comparison to the over-expression from pGLY-2. Only strains GP3 and GP4 showed improved glycolate synthesis in M9-glucose cultures in comparison to the parent strain GP0, with 20-30% higher glycolate titers at the shake flask scale (**Supplementary Figure S8a**). However, these strains did not show appreciably improved DHBA and 3HBL synthesis (**Supplementary Figure S8b**). While we have not evaluated all possible knockout combinations exhaustively, these results suggest that over-expression of *ycdW*, *aceA* and *aceK* alone allows sufficient glycolate synthesis in the base strain GP0, with glycolate and glyoxylate consumption not being significantly limiting at the shake flask scale. These preliminary observations warrant a more detailed study of these and other engineered strains at the bioreactor scale.

Supplementary Methods

Supplementary Table S1 | List of DNA oligonucleotide primers used in the cloning of genes and for qPCR reactions

Primer names correspond to the name of the gene or vector backbone that the primer amplifies, whether the primer is the forward primer (FP) or reverse primer (RP) of that gene or vector, and the restriction site incorporated into the primer sequence (in case of a primer used to generate a fragment for cloning). For primers used to amplify the *acs* and *tesB* genes from *E. coli* for the construction of the *acs-tesB* operon, sequences indicated in bold correspond to parts of the complementary overlapping regions for SOEing PCR.

Primer	Sequence 5'→3'	Source
ycdW-FP-NdeI	TAAAAACATATGGATATCATCTTTTATCACCCAACG	Sigma-Genosys
ycdW-RP-XhoI	TAAAAACTCGAGTTAGTAGCCGCGTGCG	Sigma-Genosys
aceAK-FP-NcoI	TAAAAACCATGGGCATGGAGCATCTGCAC	Sigma-Genosys
aceAK-RP-EcoRI	TAAAAAGAATTCTCAAAAAAGCATCTCCCCATAC	Sigma-Genosys
pETDuet-ΔT7-FP-XmaI	GAAAAAACCCGGGGGCAGATCTCAATTGGATATCGG	Sigma-Genosys
pETDuet-ΔT7-RP-XmaI	GAAAAAACCCGGGGATCTCGATCCTCTACGCCG	Sigma-Genosys
pCDFDuet-ΔT7-FP-XmaI	GAAAAAACCCGGGGGCAGATCTCAATTGGATATCGG	Sigma-Genosys
pCDFDuet-ΔT7-RP-XmaI	GAAAAAACCCGGGGAGTCGCATAAGGGAGAGCGTC	Sigma-Genosys
ycdW-qPCR-FP	CACATGTCGCCGCGATT	Sigma-Genosys
ycdW-qPCR-RP	GGCAATGGTGCGAGAAATGTA	Sigma-Genosys
aceA-qPCR-FP	ACCGGCGAGCGTACCA	Sigma-Genosys
aceA-qPCR-RP	CCAGGCCACGGCTGATC	Sigma-Genosys
NdeI-*acs*-FP	TAAAAACATATGAGCCAAATTCACAAACACAC	Sigma-Genosys
acs-RP	**TATATATCTCCTTCTTATTTACGATGGCATC**GCGATAG	Sigma-Genosys
tesB-FP	**GATGCCATCGTAAATAAGAAGGAGATATATA**ATGAGTCAGG CGATAAAAAATTTAC	Sigma-Genosys
PacI-*tesB*-RP	TAAAAAAATTAATTGTGATTACGCATCACCC	Sigma-Genosys

Supplementary Table S2 | Molar yields and selectivity in the synthesis of 3,4-DHBA and 3HBL from glucose

Supplied Glucose	Molar Yield (3,4-DHBA + 3HBL) on Glucose*	% of Theoretical Pathway Yield	$\frac{([DHBA]+[3HBL])}{[3HB]}$	$\frac{([3,4\text{-}DHBA]+[3HBL])}{([2,3\text{-}DHBA]+[3HB])}$	$\frac{([3,4\text{-}DHBA]+[3HBL])}{[2,3\text{-}DHBA]}$
8 g/L	0.112	17.0	4.93 ± 0.32	2.35 ± 0.23	5.41 ± 0.68
10 g/L	0.160	24.2	4.63 ± 0.26	1.07 ± 0.09	1.69 ± 0.18
15 g/L	0.152	23.0	4.26 ± 0.41	0.93 ± 0.07	1.48 ± 0.09

* Molar yield is calculated as ratio of moles of 3,4-DHBA + 3HBL synthesized to moles of glucose consumed and does not include 2,3-DHBA. The total molar pathway yield values including 2,3-DHBA are 0.148, 0.285 and 0.274 respectively for 8, 10 and 15 g/L of supplied glucose and amount to 22.4%, 43.2% and 41.5% of the theoretical maximum yield.

Supplementary Table S3 | Product Titers (mM) for different concentrations of supplied glucose

Supplied Glucose	3,4-DHBA (mM)	3HBL (mM)	2,3-DHBA (mM)	3HB (mM)	Glycolate (mM)	Acetate (mM)	Unconsumed Glucose (mM)
8 g/L	3.1 ± 0.2	1.9 ± 0.2	0.9 ± 0.1	2.35 ± 0.5	2.0 ± 0.1	5.2 ± 0.5	0.0 ± 0.0
10 g/L	5.8 ± 0.9	3.1 ± 0.1	5.3 ± 0.5	1.07 ± 1.0	3.1 ± 0.1	11.0 ± 1.2	0.0 ± 0.0
15 g/L	5.4 ± 0.5	3.0 ± 0.1	5.7 ± 0.6	0.93 ± 2.4	3.4 ± 0.7	13.4 ± 0.4	27.1 ± 3.5

Supplementary Table S4 | Molar distribution of supplied glucose in the synthesis of different products*

Supplied Glucose	Glucose for 3,4-DHBA + 3HBL (mM)	Glucose for 2,3-DHBA (mM)	Glucose for 3HB (mM)	Glucose for Glycolate (mM)	Glucose for Acetate (mM)	Unconsumed Glucose (mM)	Glucose for B&M** (mM)
8 g/L (44.4 mM)	5.0	0.9	1.2	8.4	2.6	0	26.3
10 g/L (55.5 mM)	8.9	5.3	3.1	4.6	5.5	0	28.2
15 g/L (83.3 mM)	8.4	5.7	3.4	4.3	6.7	27.1	27.7

* The glucose consumed theoretically in the formation of each of the products in the above table is estimated using the product titers from **Supplementary Table S3** and the stoichiometric coefficients from the above listed theoretical reactions.

** Glucose for B&M = Glucose for Biomass and Maintenance functions and is calculated as the difference between the supplied glucose and the sum of the glucose consumed theoretically for the formation of different products and the unconsumed glucose.

Supplementary Calculations

Net Reactions and Theoretical Yield Calculations - Synthesis of DHBA, 3HBL and other products from glucose

Calculation of pathway independent theoretical maximum yield on glucose (Y^E)

The pathway independent maximum yield (Y^E), is a measure of the most efficient conversion of a given substrate into a product along a hypothetical (or real) route that is redox neutral and hence captures all the energy of the starting substrate into the product (Dugar and Stephanopoulos, 2011). For DHBA synthesis from glucose, the net reaction for this conversion is:

~~4 moles Glucose ⟶ 3 moles 3,4-DHBA~~

~~Thus, Y^E = 4/3 = 1.33 moles DHBA / mole of glucose~~

2 moles Glucose ⟶ 3 moles 3,4-DHBA

Thus, Y^E = **Degree of reductance for glucose / degree of reductance of 3,4-DHBA**
= (6x4 + 12x1 – 6x2) / (4x4 + 8x1-4x2)
= 24/16 = 1.5 moles DHBA / mole of glucose

Calculation of maximum theoretical pathway yield (Y^P)

Pathway Reactions (without acetate recycling)

Glycolate synthesis:

½ Glucose + ADP + P_i + $3NAD^+$ + FAD + NADPH + CoASH ⟶ Glycolate + CO_2 + ATP + $FADH_2$ + 3NADH +NADP + CoASH

DHBA / 3HBL synthesis:

Glucose + Glycolate + 2ADP + 2P_i + $4NAD^+$ + NADPH + 2CoASH ⟶ 3,4-DHBA + 2CO_2 + Acetate + 2ATP + 4NADH + NAPD + 2CoASH

Net Reaction:

3/2 Glucose + 3ADP + 3P_i + $7NAD^+$ + 2NADPH +FAD+ 3CoASH ⟶ 3,4-DHBA + 3CO_2 + Acetate + 3ATP + + 7NADH +2NAPD +$FADH_2$ + 3CoASH

Theoretical pathway yield $Y^P_{w/o\text{-}acetate\text{-}recycling}$ **= 0.67 moles 3,4-DHBA / mole of glucose**

The net reaction above shows that the pathway results in the synthesis of an excess of reducing equivalents which affect the overall yield. Separate reactions for regeneration of NADPH are not taken into account, assuming that the excess of NADH synthesized can supply some of the NADPH requirement through inter-conversion by transhydrogensases.

For every mole of 3,4-DHBA synthesized, a mole of acetate is formed as a by-product. The pathway above also shows an excess of reducing equivalents and ATP synthesis. Recycling acetate into acetyl-CoA by activation with acetyl-CoA synthetase (Acs) using this excess of ATP can help improve the maximum theoretical pathway yield as below.

Pathway Reactions (with acetate recycling)

Net Reaction:

Glucose + ADP + P_i + $5NAD^+$ + 2NADPH + FAD + 2CoASH ⟶ 3,4-DHBA + $2CO_2$ + ATP + 5NADH + 2NAPD + $FADH_2$ + 2CoASH

Theoretical pathway yield $Y^P_{with\text{-}acetate\text{-}recycling}$ **= 1.0 moles 3,4-DHBA / mole of glucose**

3HB synthesis reaction:

Net Reaction:

Glucose + 2ADP + $2P_i$ + $4NAD^+$ + NADPH + 4CoASH ⟶ 3HB + $2CO_2$ + 2ATP + 4NADH + NAPD + 4CoASH

2,3-DHBA synthesis reaction:

Net Reaction:

3/2Glucose + ADP + P_i + $5NAD^+$ + 2NADPH + FAD + 2CoASH ⟶ 2,3-DHBA + $2CO_2$ + ATP + 5NADH + 2NAPD + $FADH_2$ + 2CoASH

Supplementary References

Dugar, D., Stephanopoulos, G., 2011. Relative potential of biosynthetic pathways for biofuels and bio-based products. Nature Biotechnology. 29**,** 1074-1078.

Martin, C. H., Dhamankar, H., Tseng, H.-C., Sheppard, M. J., Reisch, C. R., Prather, K. L. J., 2013. A platform pathway for production of 3-hydroxyacids provides a biosynthetic route to 3-hydroxy-gamma-butyrolactone. Nature Communications. 4**,** 1-7.

Soucaille, P., Glycolic acid production by fermentation from renewable resources. In: Office, U. S. P., (Ed.), United States, 2009.